

2012年電波航法研究会

津波に対するレーダ観測活動の
調査(その2)

平成24年9月7日
元日本工業大学
渡辺康夫

調査(その2)の構成

1. はじめに
2. 衛星搭載マイクロ波電波高度計の津波観測
東北太平洋沖地震津波: merging tsunami
3. HFレーダの津波観測
東北太平洋沖津波: tsunami signal
4. 津波探知のためのスペースセンサ
GNSS-Rを応用した津波探知技術等
5. おわりに
論文等資料

Fig. 1 2004 Indian Ocean Tsunami

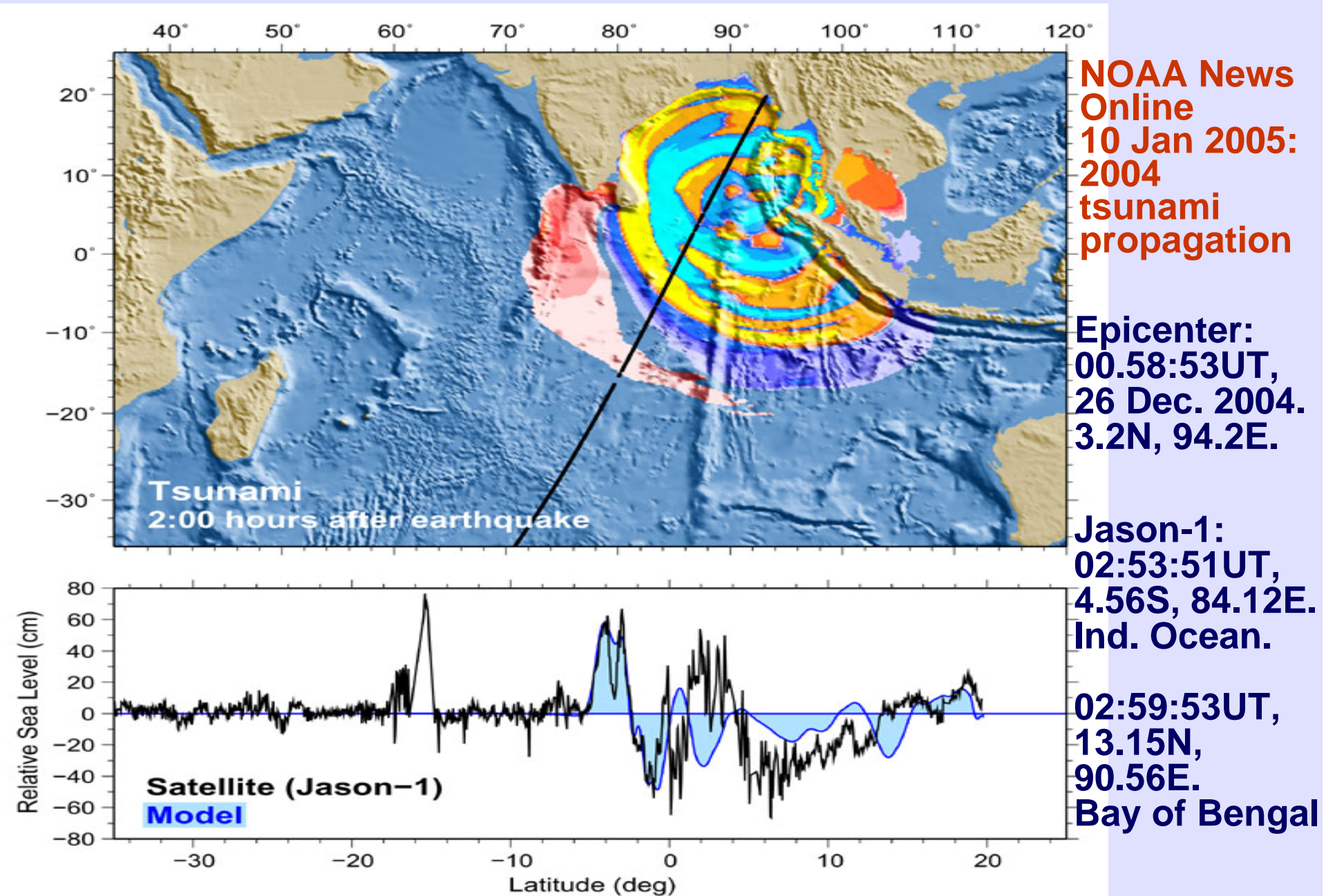
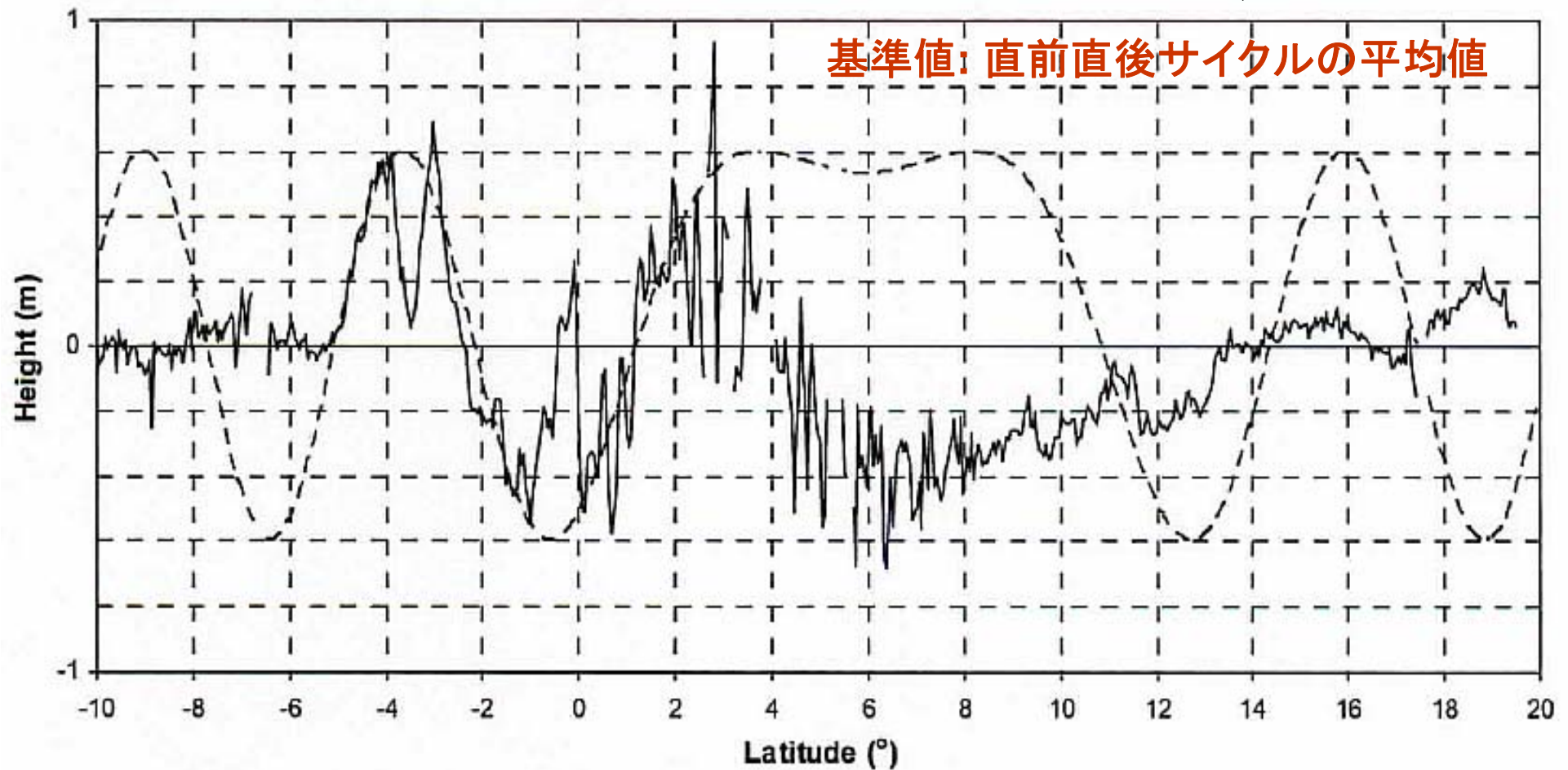


Fig. 2 Sea Surface Height Anomalies: Data by Jason-1 and Model

Gower, Int. J. Remo
Sens, 2007



Solid: corrected sea surface height: (1) 4.56S: $h=70\text{cm}-(30-40)\text{cm}$,
peak-to-peak 1m. (2) 13.15N: $h=-20\text{cm}$. (3) $v=739\text{km/h}$ for
av. depth=4300m.

Dotted: sine wave model with $\lambda = 580\text{km}$, $v=739\text{km/h}$, $h=0.6\text{m}$.

Fig. 3 Tsunami Shadows

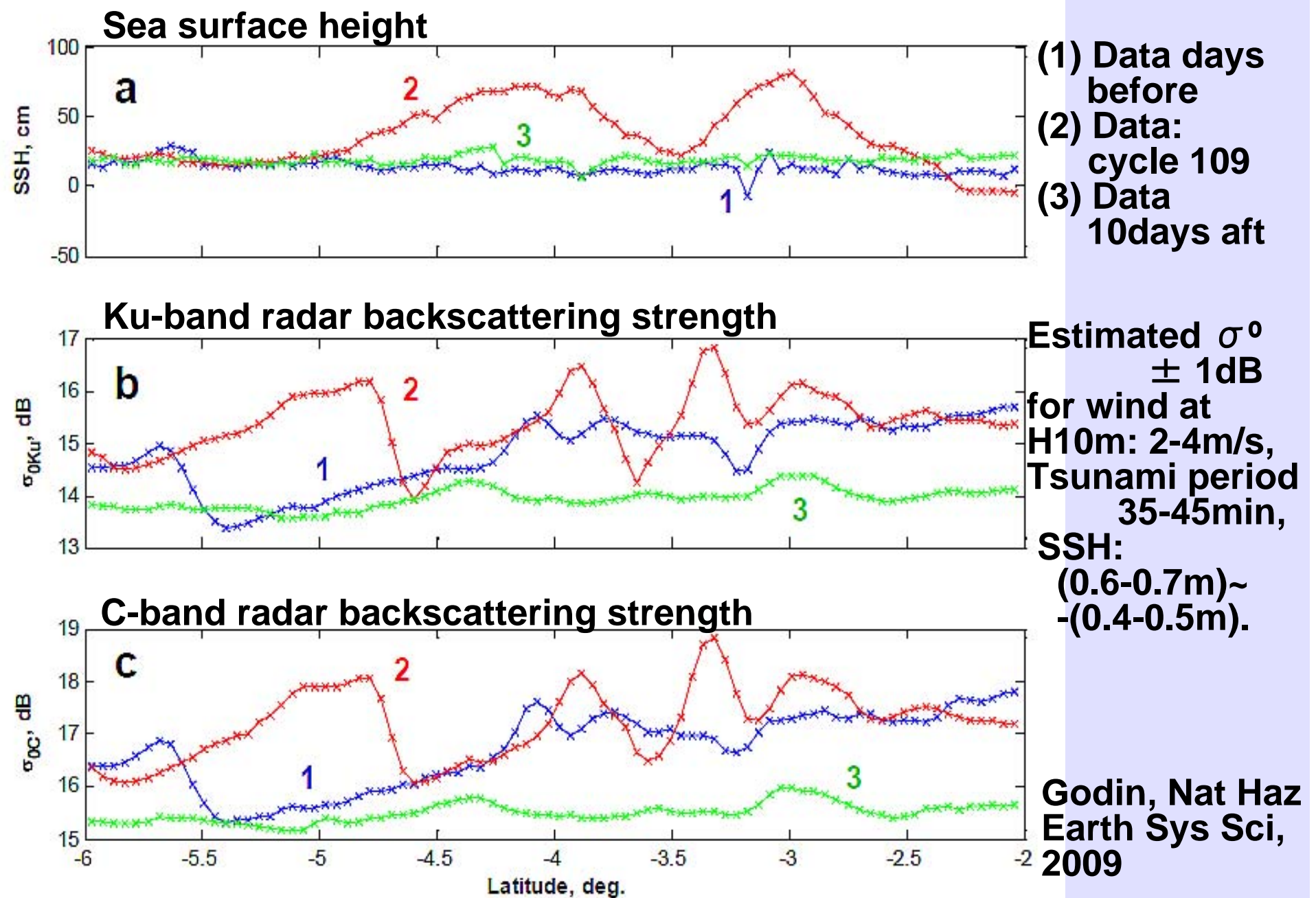
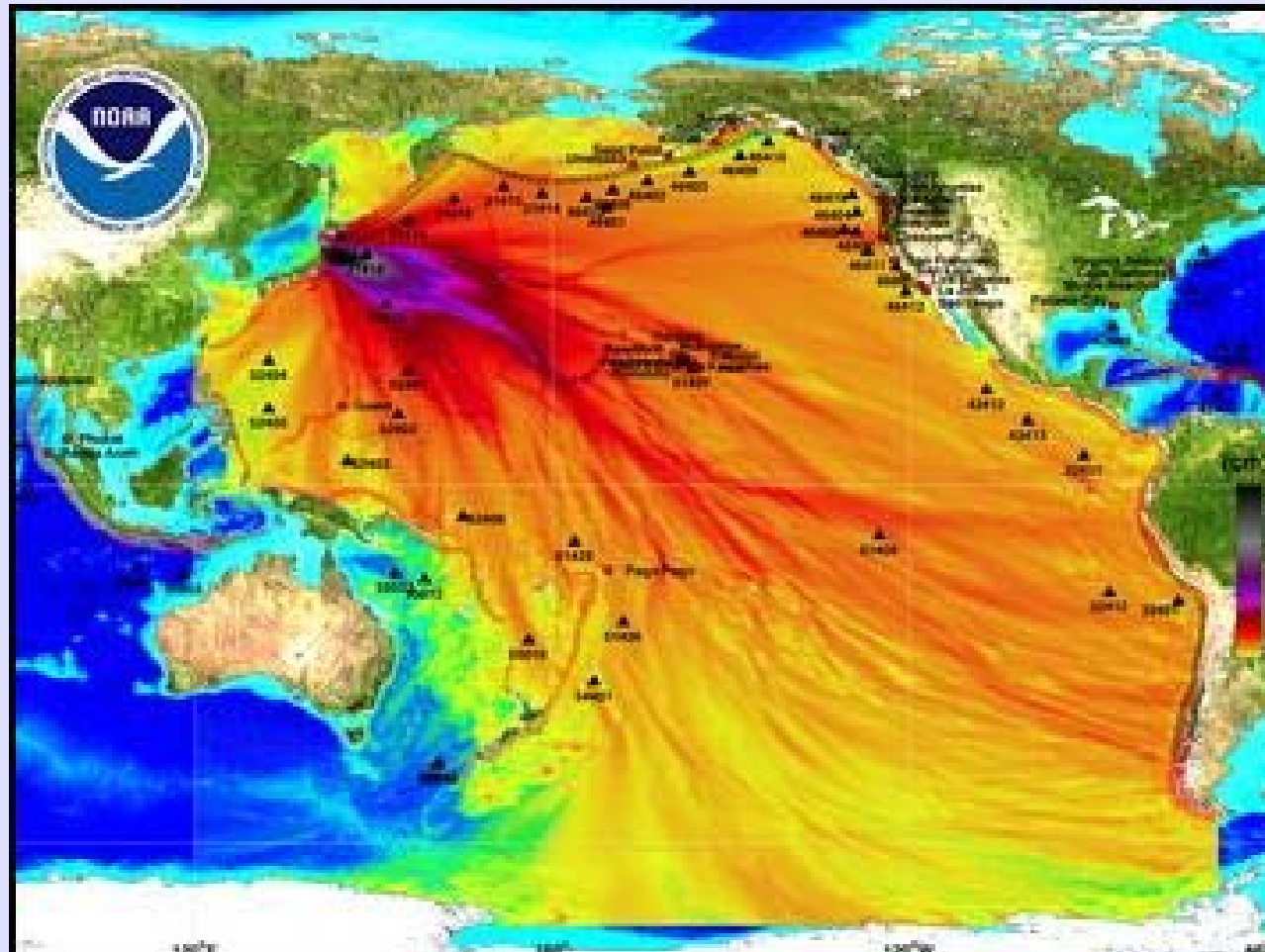
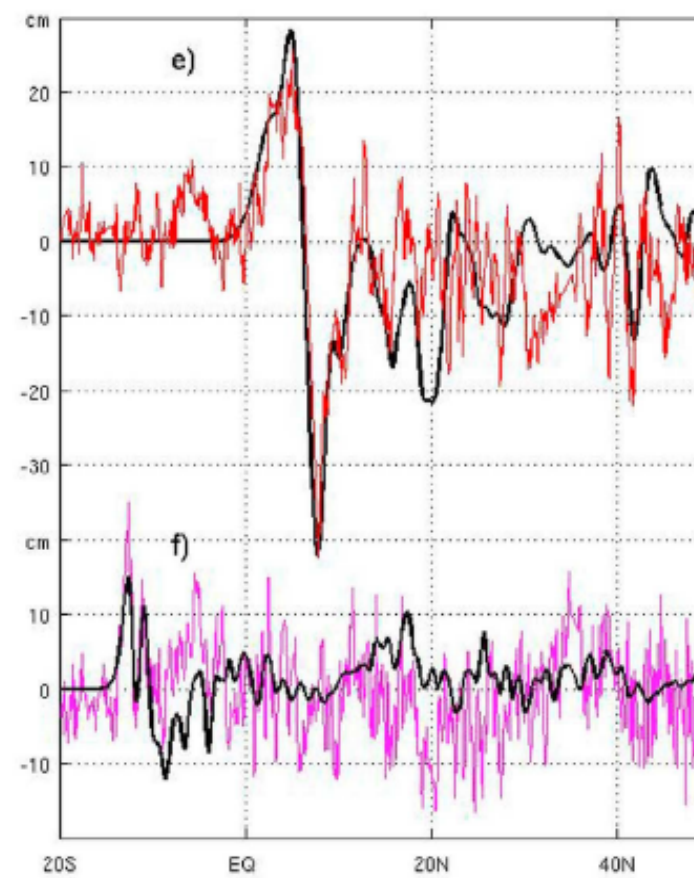
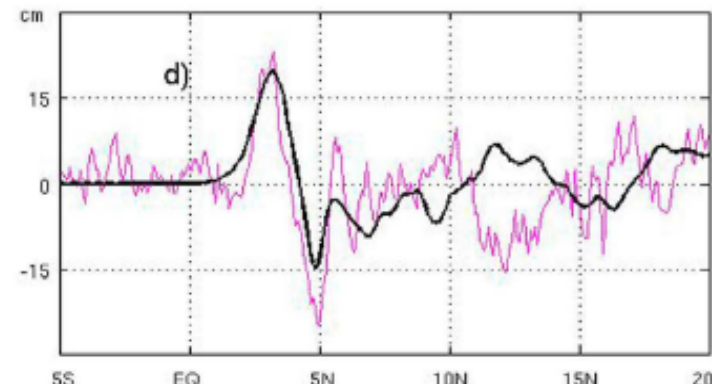
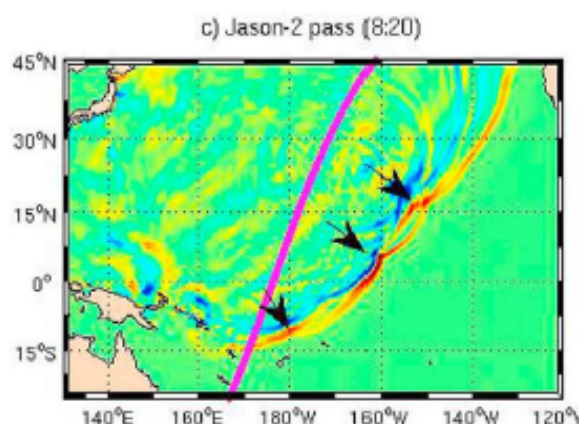
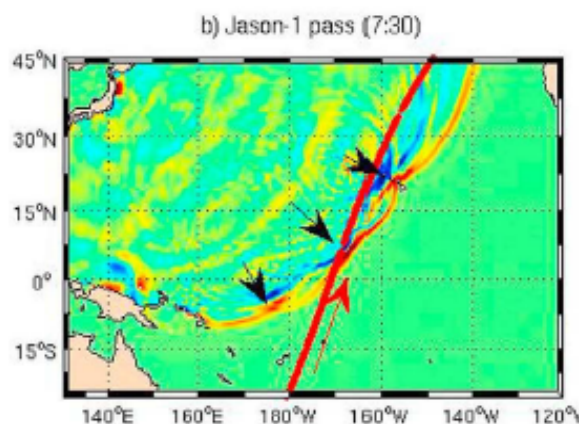
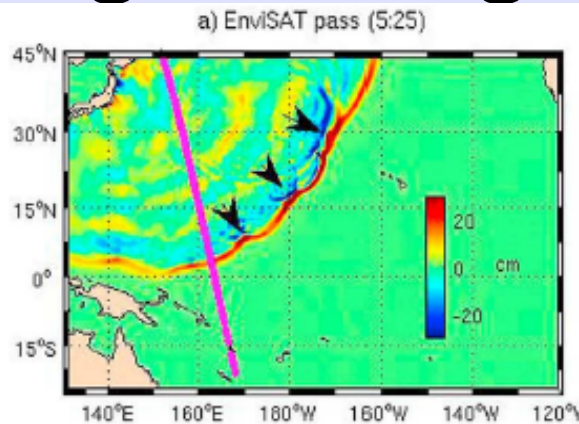


Fig. 4 Japan Tsunami, 11 March 2011



<http://nctr.pmel.noaa.gov/>

Fig. 5 Merging Tsunami, March 11, 2011



- a) ENVISAT at 5:25 after quake
- b) Jason-1 at 7:30 after
- c) Jason-2 at 8:20 after
- d) Tsunami model (black) and ENVISAT data
- e) Jason-1 over Mid-Pacific Mt. Merging tsunami (red arrow)
- f) Jason-2 data

Black arrows:
locations of
merging tsunamis

**Fig. 6 Tsunami Model. (a) Amplitude
(b) Amplitude (blue lines), Bathymetry (color bar)**

Song, Geo Res
Let, 2012

Crosses:DART

Black arrows:
tsunami jets fr.
ES:Emperor
Seamounts
nwHR:N-west
Hawaiian Ridge
HR:Hawaiian R
Mid-Pacific Mt
MI:Martial Is
ME:Mendocino
Escarpments

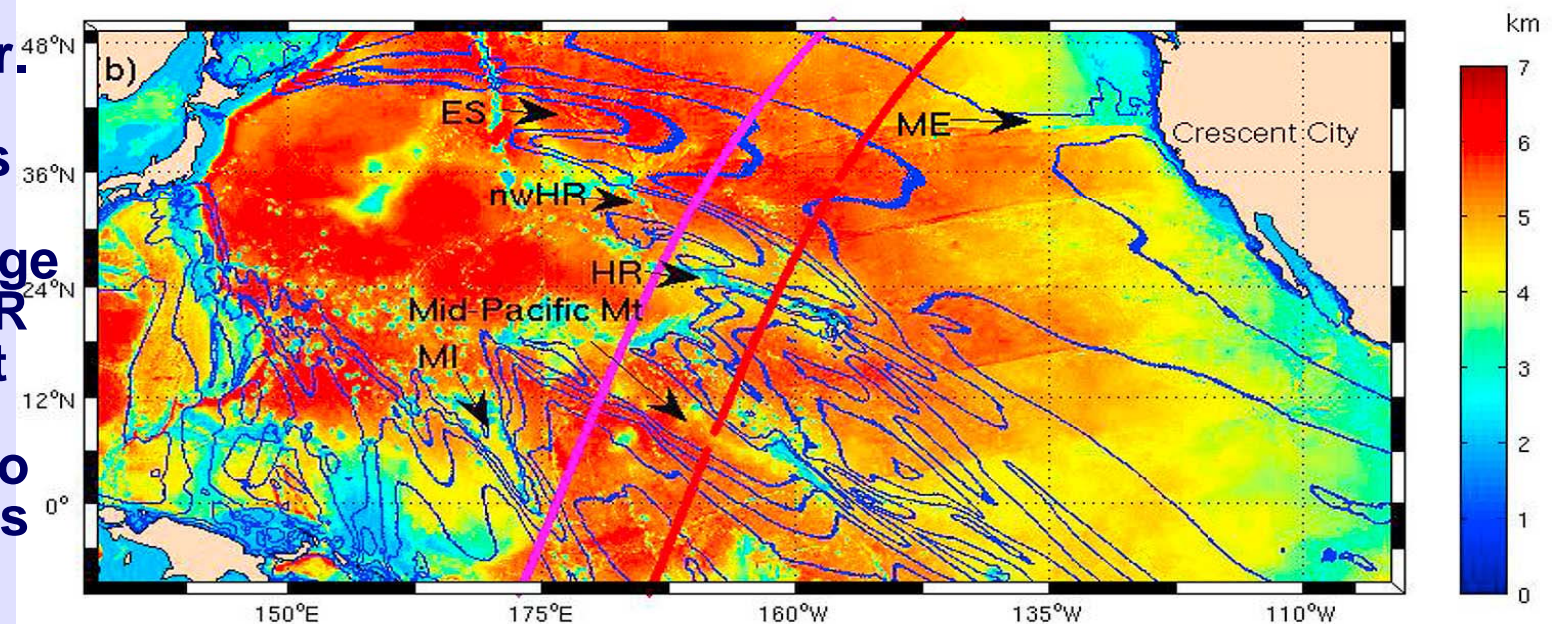
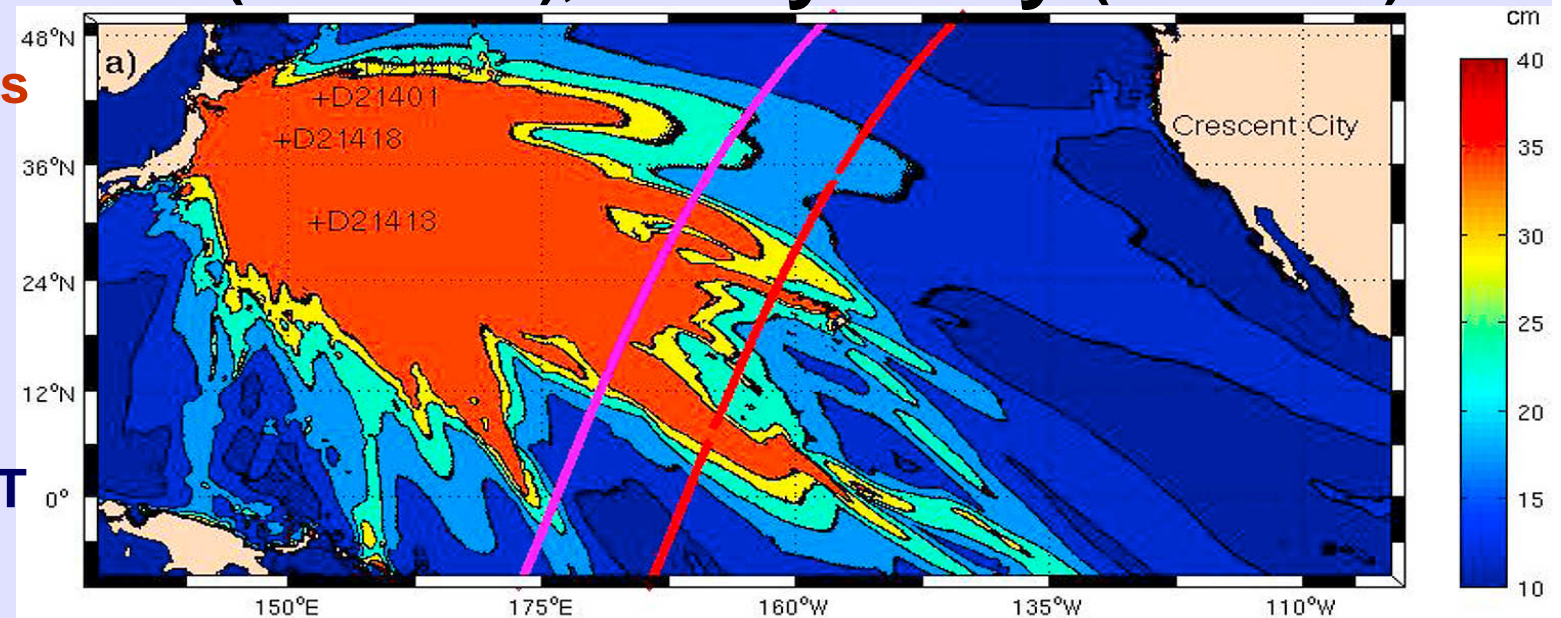
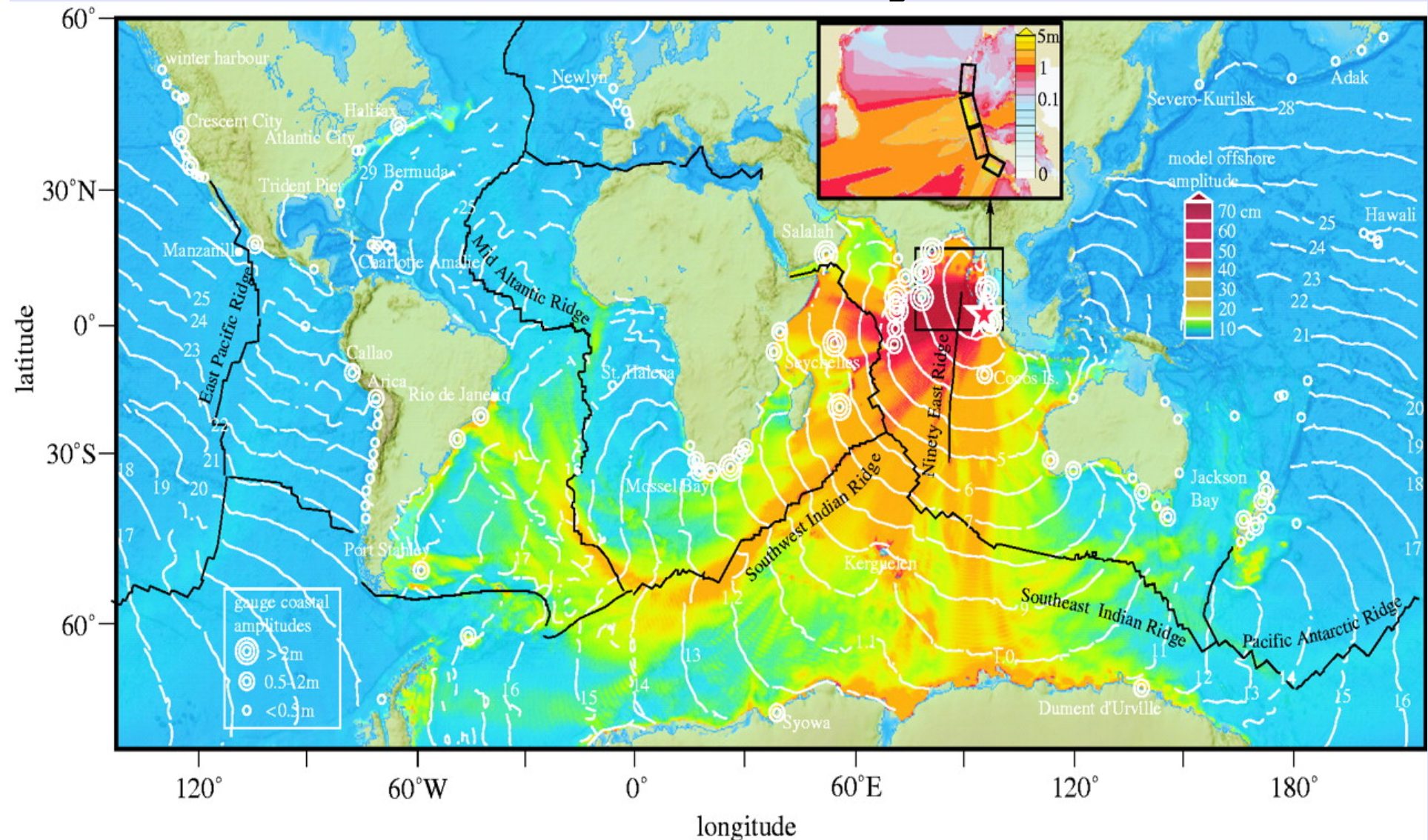


Fig. 7 Max. Amplitude of the 26 Dec. 2004 Tsunami Modelled by Titov et al.



Titov et al., Science, 309, 23 Sept. 2005

Fig. 8 GPS-measured Land Displacement and the Derived Seafloor Displacement

Song et al., Geo Res Lett, 2012

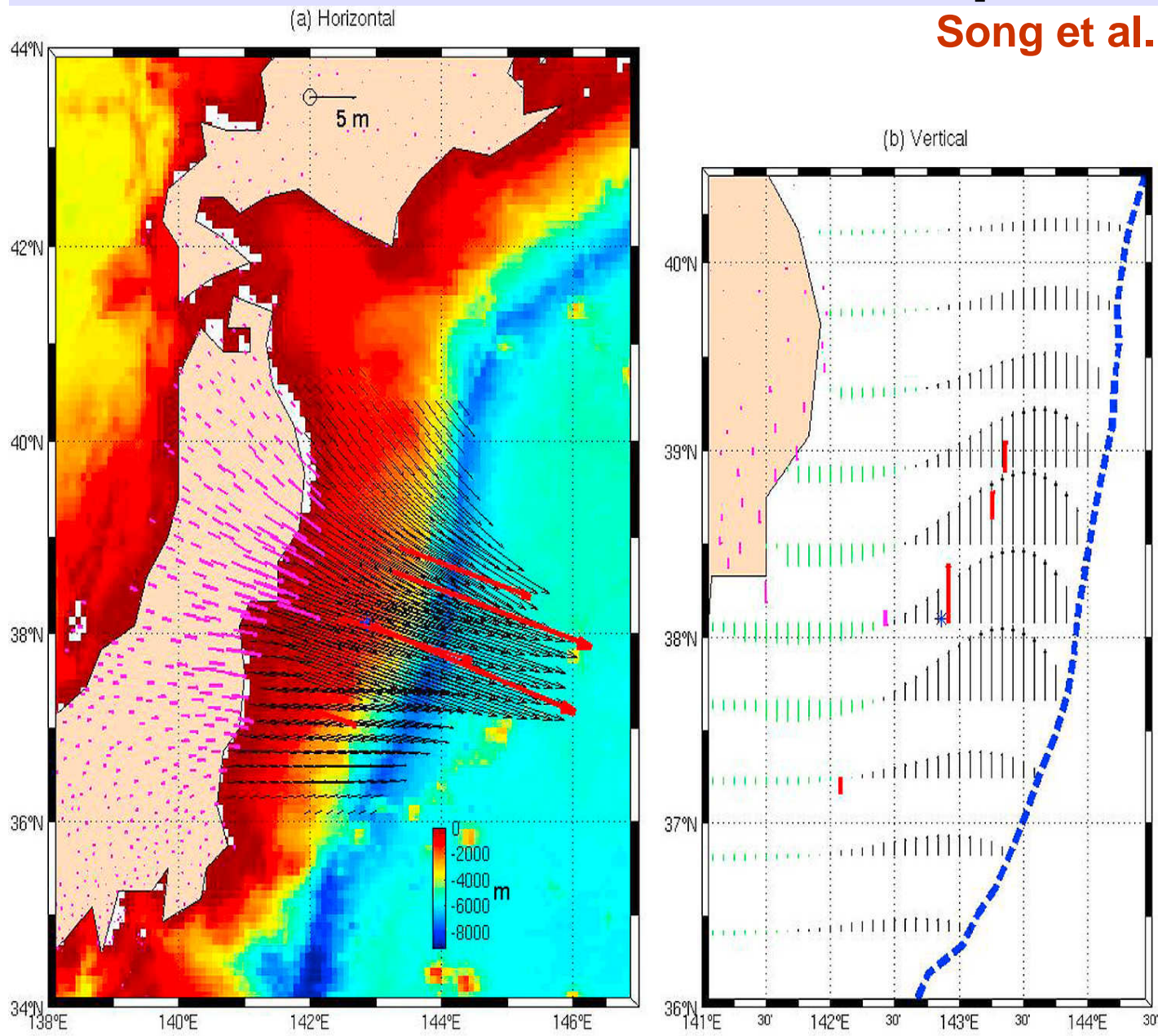
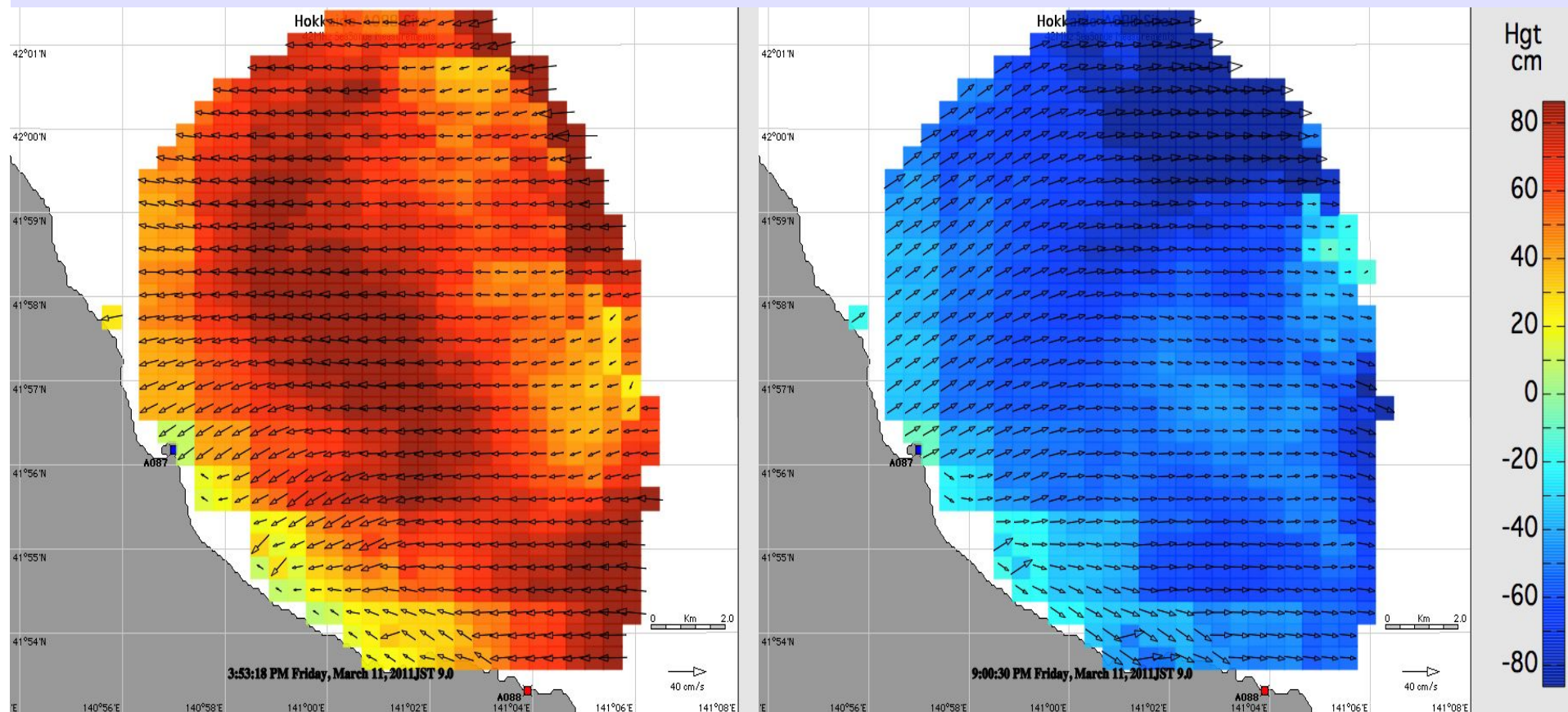


Fig. 9 Tsunami Height Superimposed on Total Current Velocity Field Measured by Radars at Usujiri and Kinaoshi



(L) Tsunami sweeping in, 15:53 JST. (R) sweeping out, 21:00 JST.
Blue dot: Usujiri, Red dot: Kinaoshi. v_0/div : 40cm/s. h: color code.

Fig. 10 Radial Current Velocities from Usujiri Radar

Lipa et al., Remote Sensing, 2012

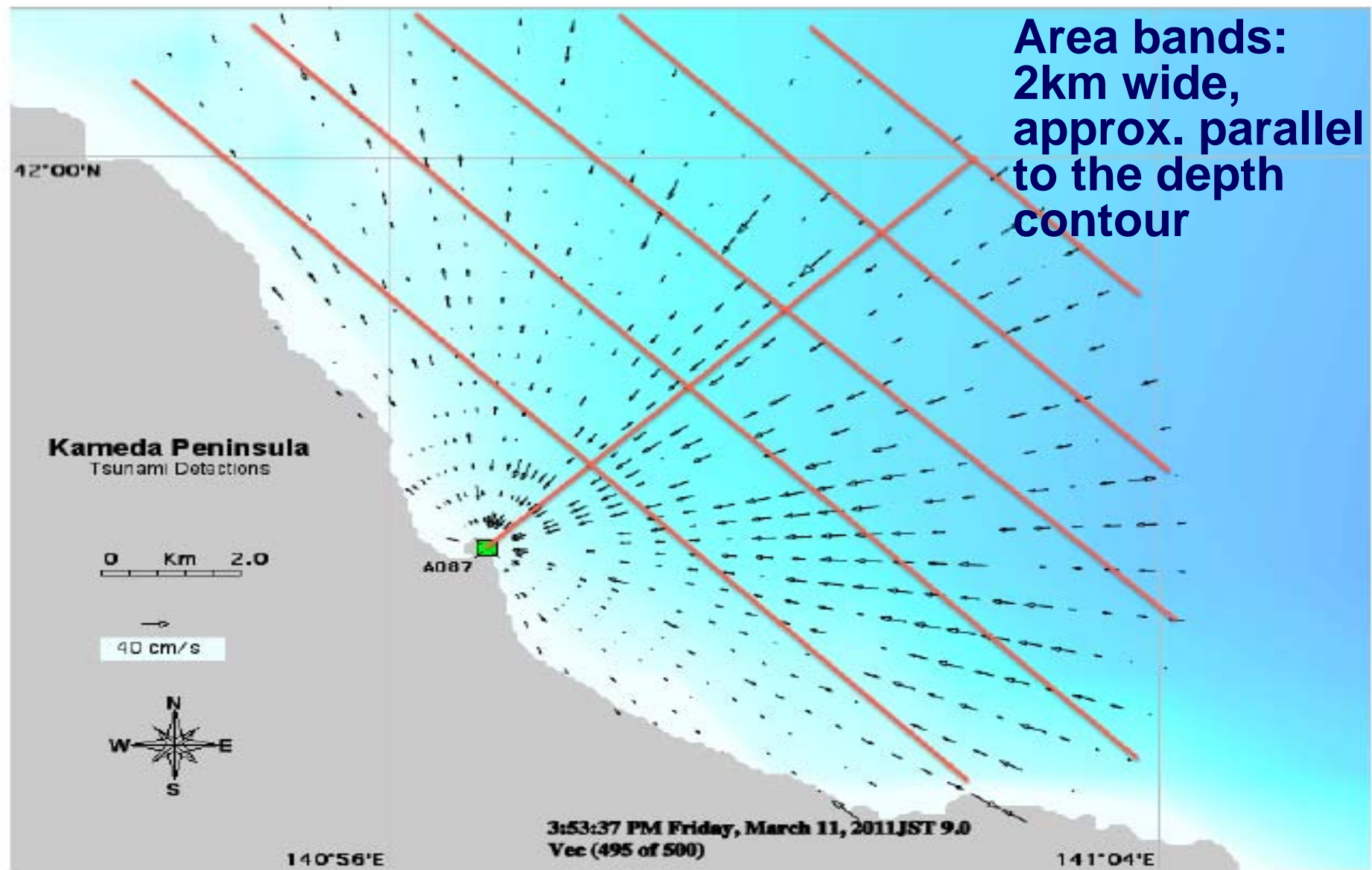
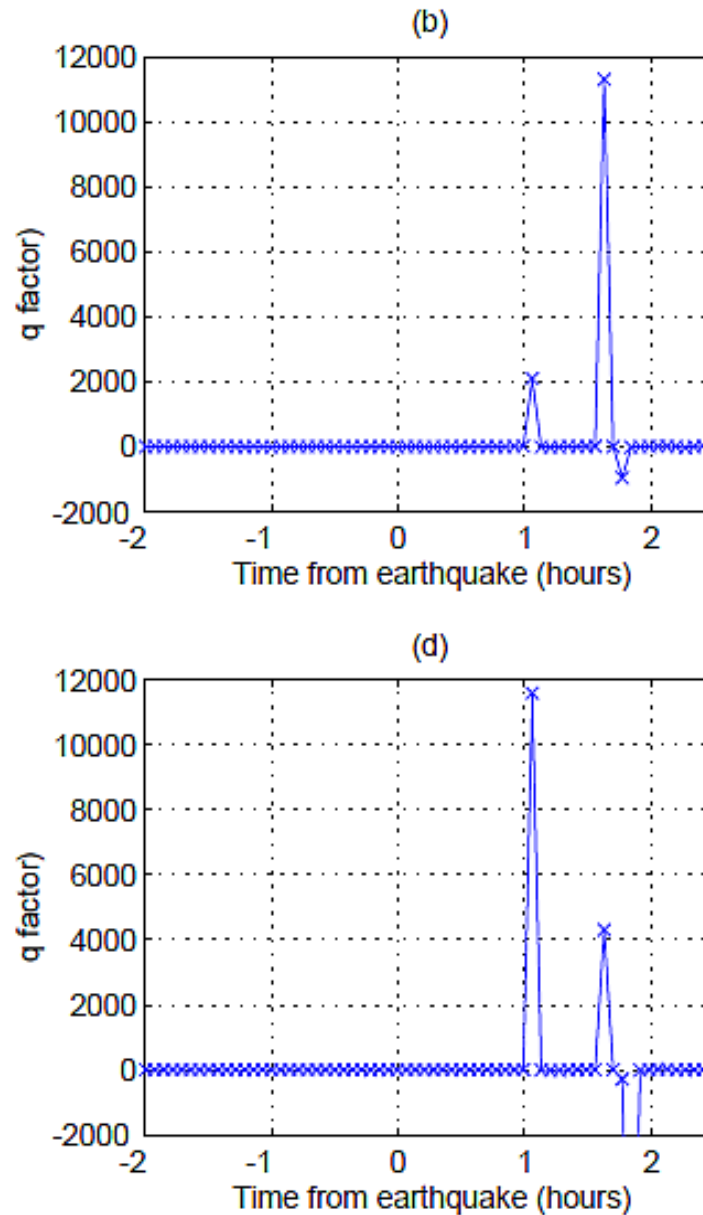
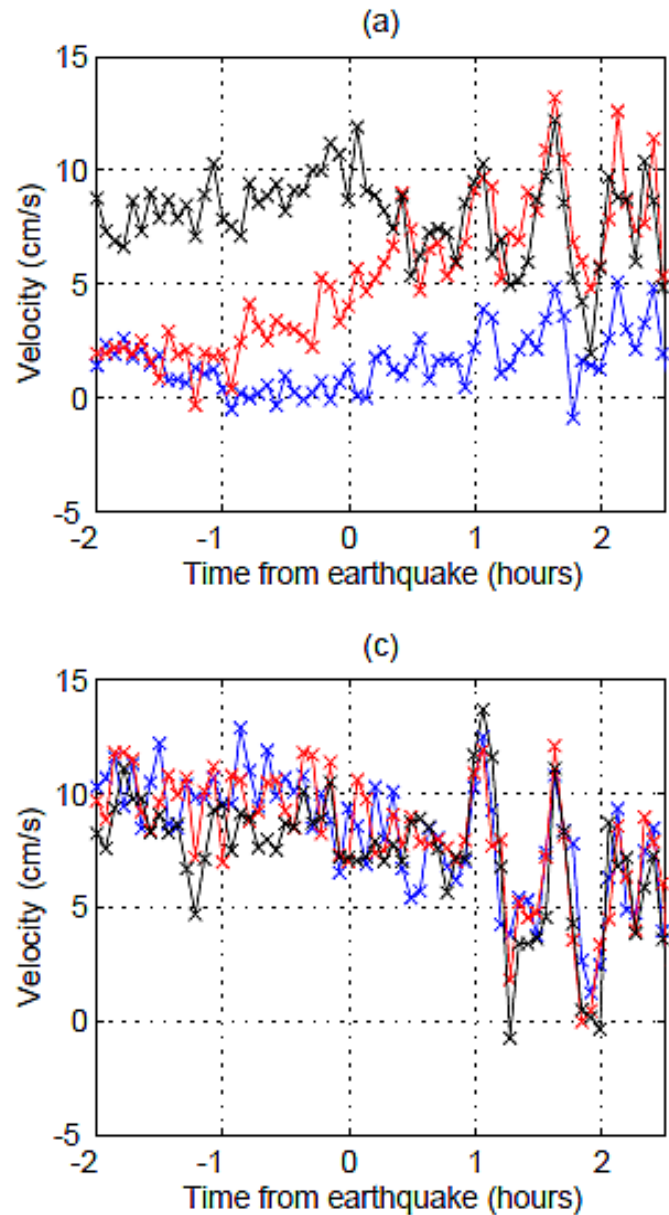


Fig. 11 Velocity Components from Kinaoshi Radar and q-factor



(a)
blue: 0-2km
red: 2-4km
black: 4-6km

(b)
Q-factor
for 0-6km

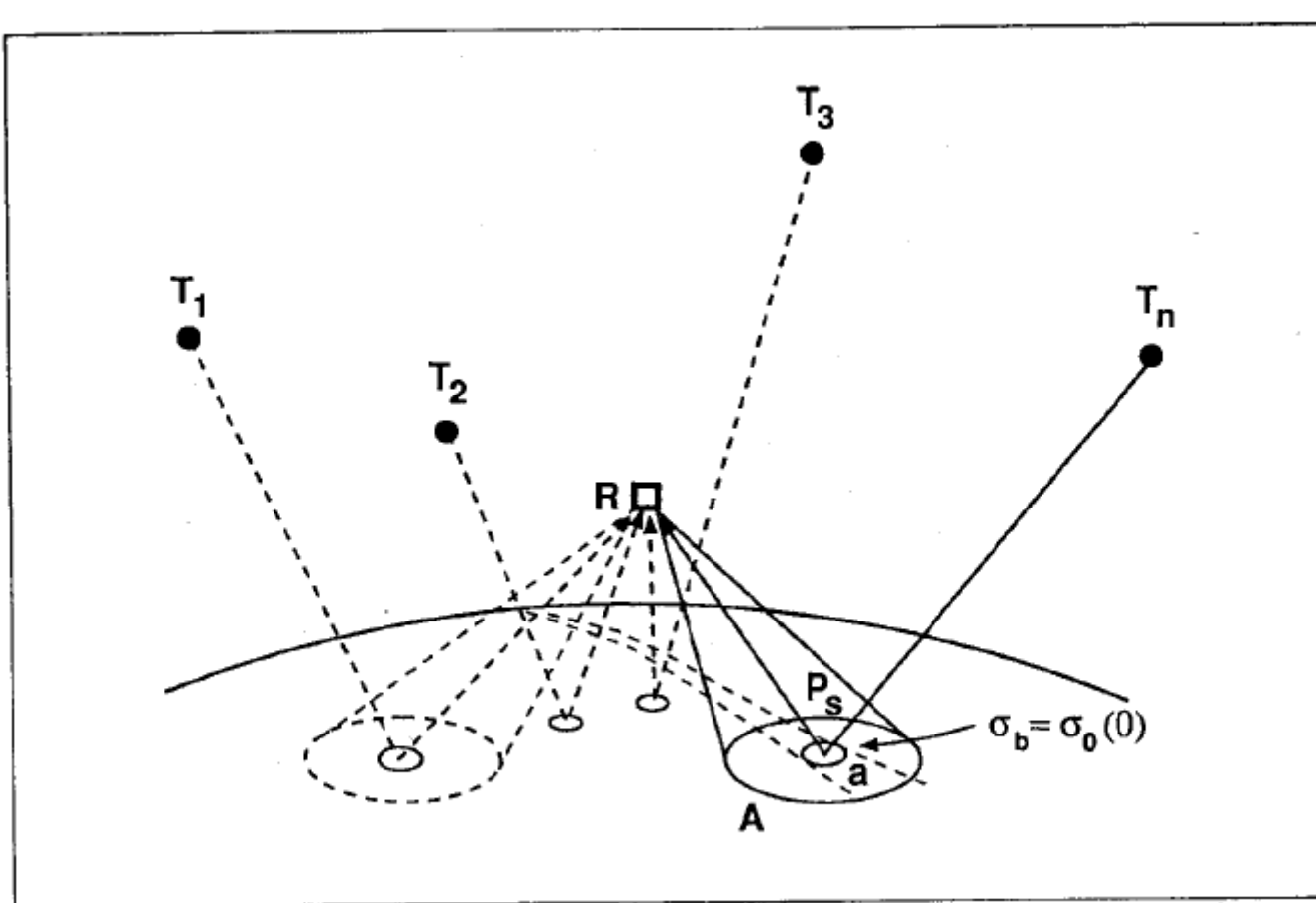
(c)
blue:6-8km
red: 8-10km
black:10-
12km

(d) q-factor
for 6-12km

Lipa, Remote
Sensing, 2012

Fig. 12 Overall System with PARIS Concept

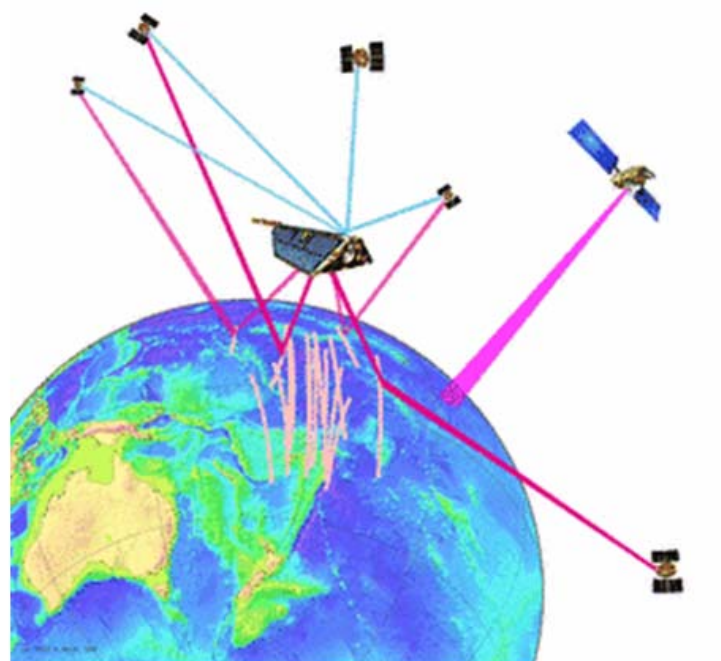
PARIS: Passive Reflectometry and Interferometry System



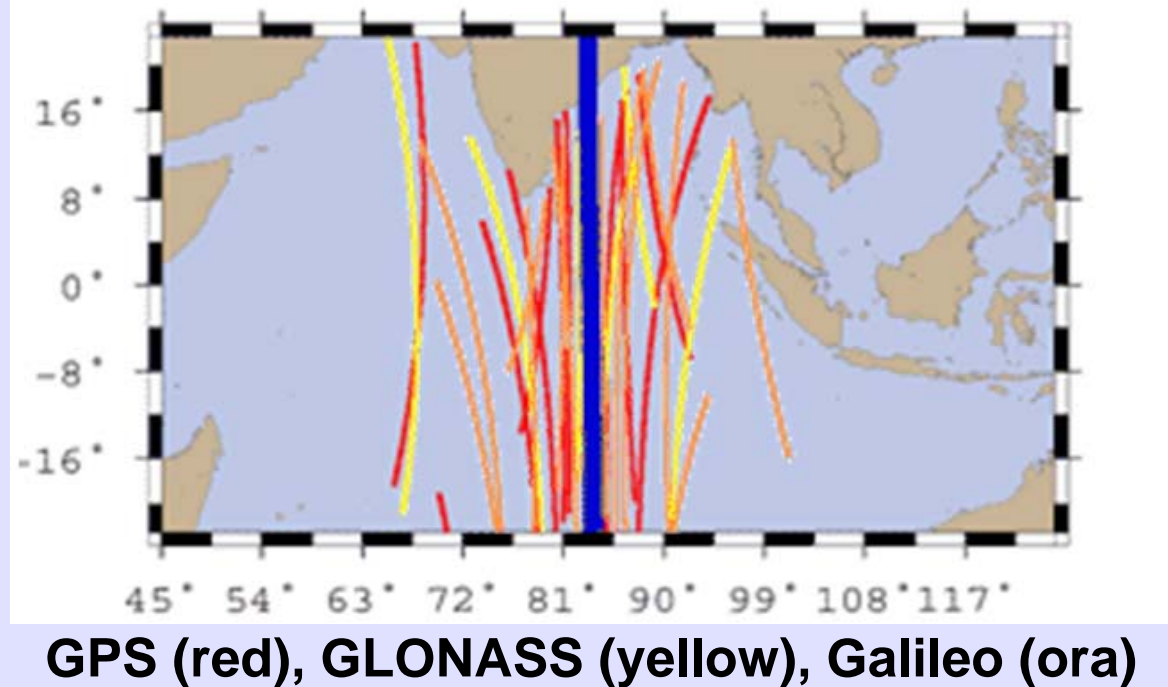
R: receiver
T: source
Number of reflections
= Number of sources

Fig. 13 Tsunami Warning Study based on GNSS-R LEO Constellation

GPS Occultation,
Reflectometry and
Scatterometry Receiver



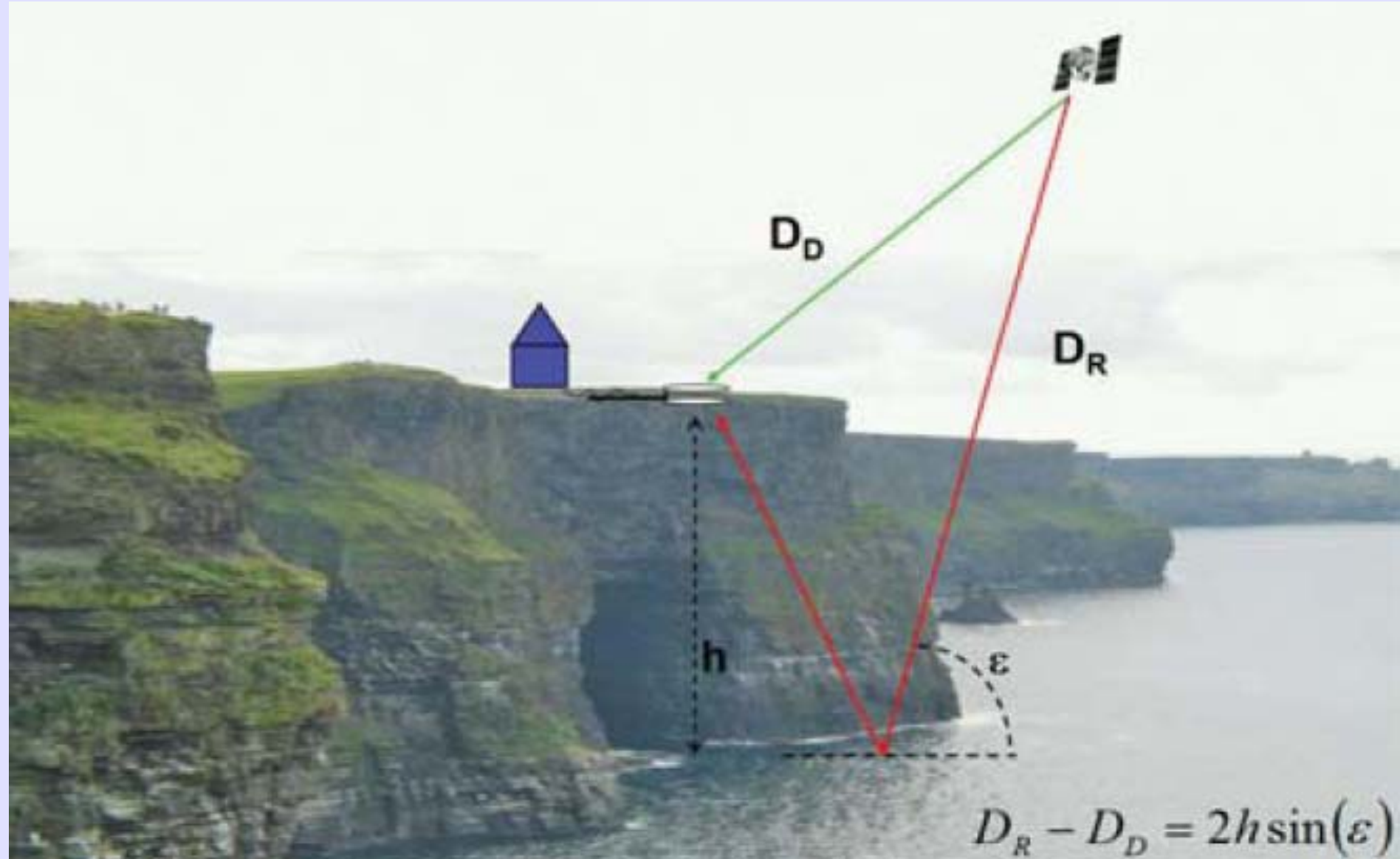
GNSS-R Reflection Points Track
(blue) at CHAMP-like LEO orbit



GNSS-R: Global Navigation Satellite System Reflectometry
LEO: Low Earth Orbit

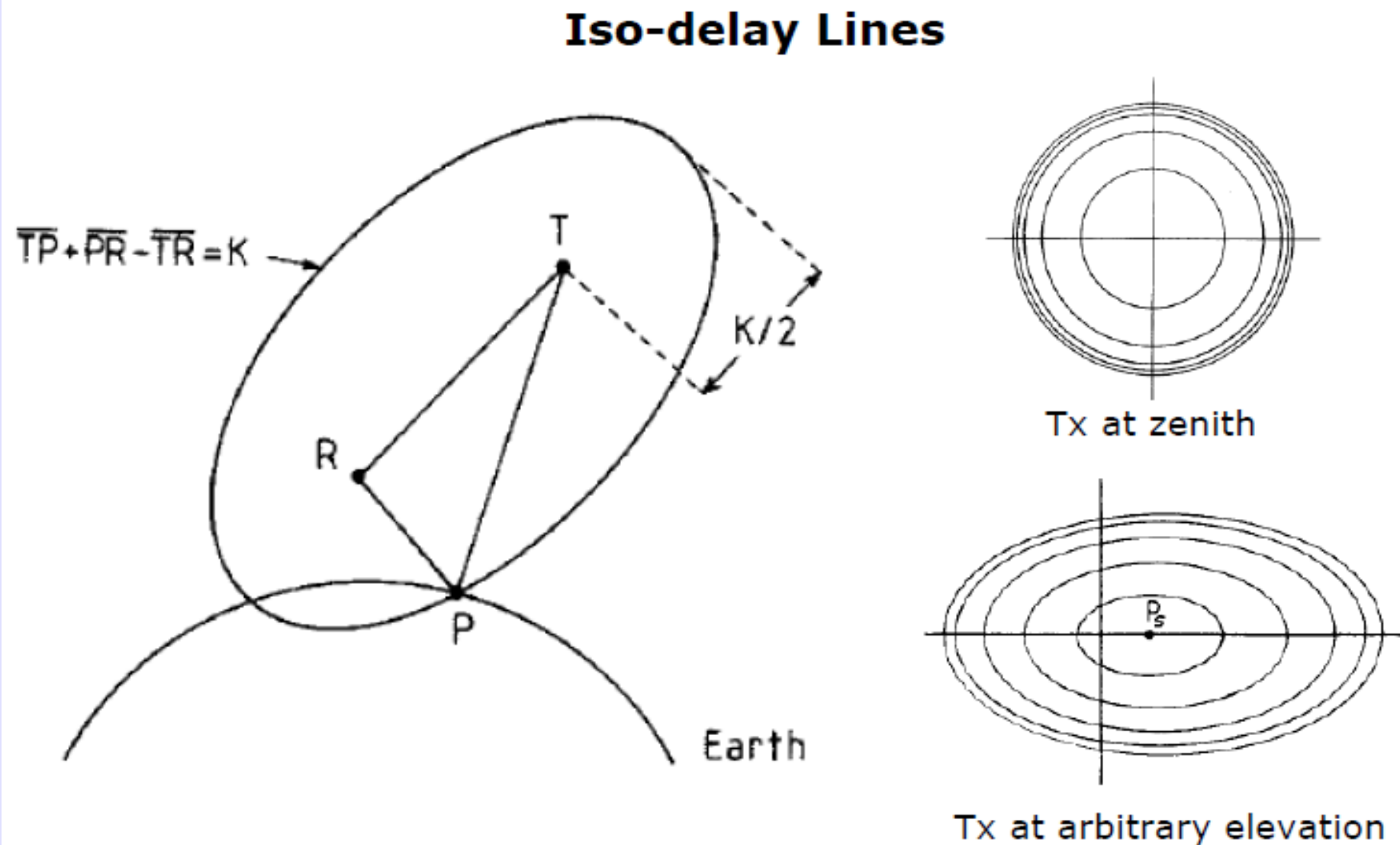
GITEWS GPS Technology, March 2012
GITEWS: German Indonesia Tsunami Early Warning System

Fig. 14 Coastal Altimetry with GNSS-R



Ruffini, IEEE Geo Remo Sens Soc Newsletter, 2006

Fig. 15 PARIS: Iso-delay lines

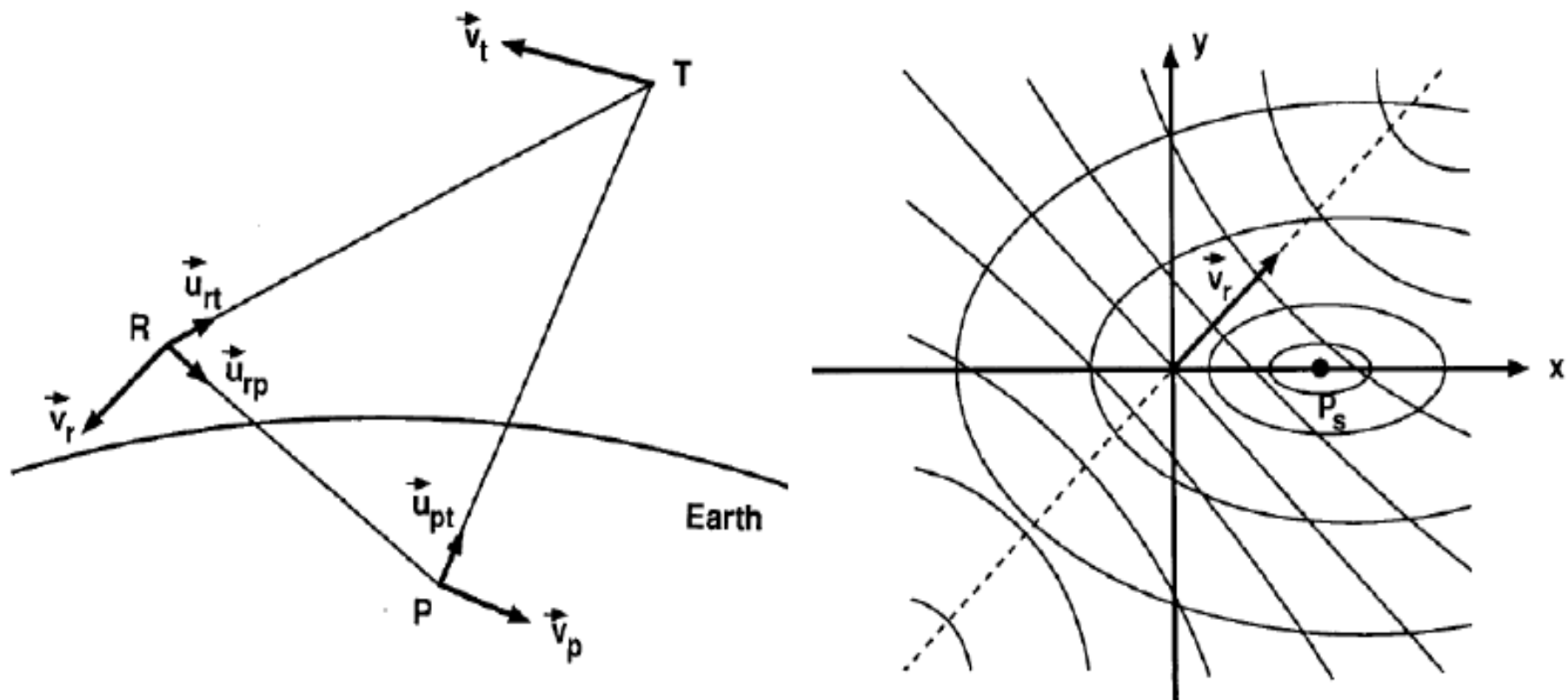


Space Reflecto 2011, Calais, France, 27-28 Oct 2011

Martin-Neira, ESA Journal, 17, 1993

Fig. 16 PARIS: Iso-Doppler Lines

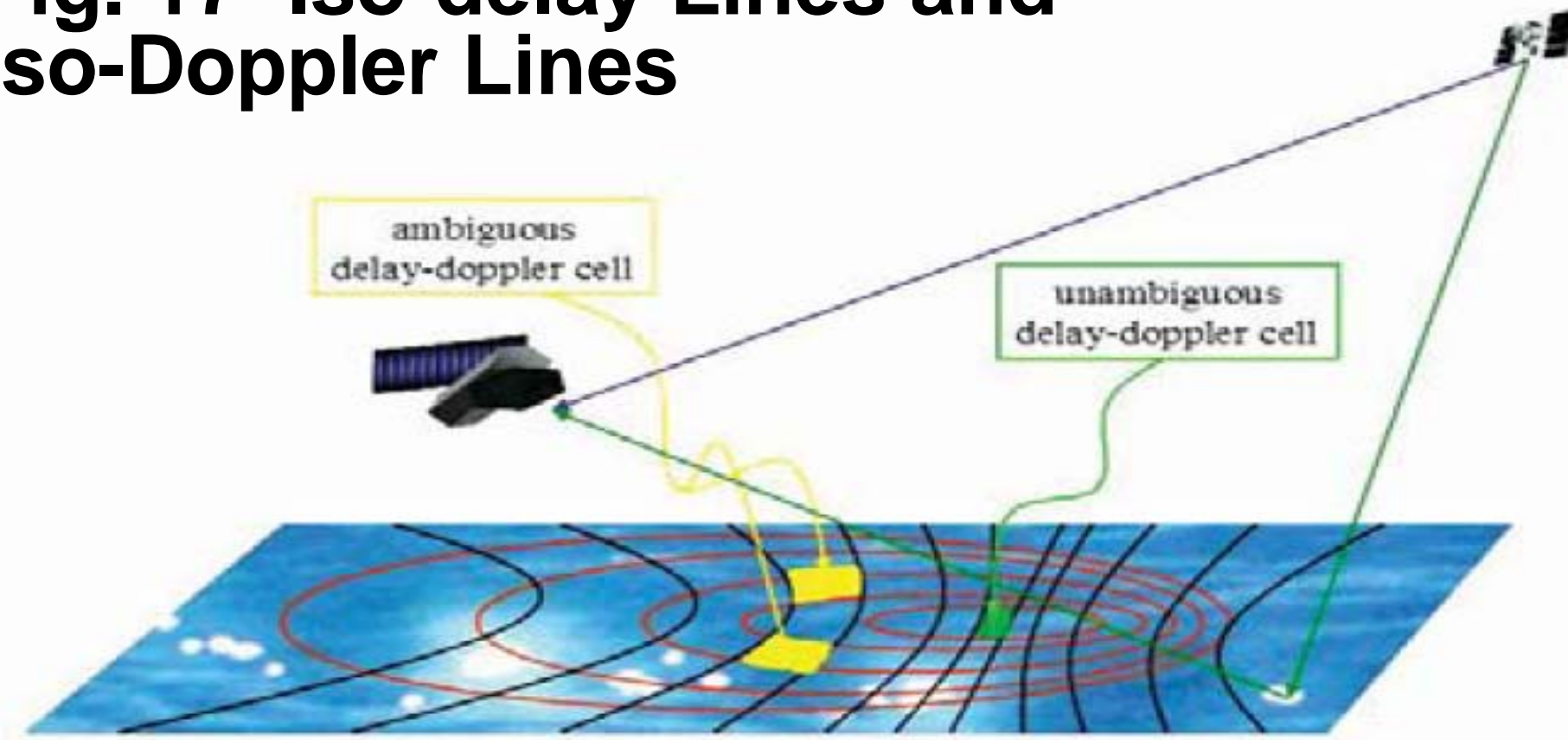
Iso-Doppler Lines



$$\vec{v}_r \bullet \vec{u}_{rp} = k_D$$

Martin-Neira, ESA Journal, 17, 1993

Fig. 17 Iso-delay Lines and Iso-Doppler Lines



Direct and reflected waveform produced by cross-correlation with clean replica

Ruffini, IEEE Geo Remo Sens
Soc Newsletter, 2006

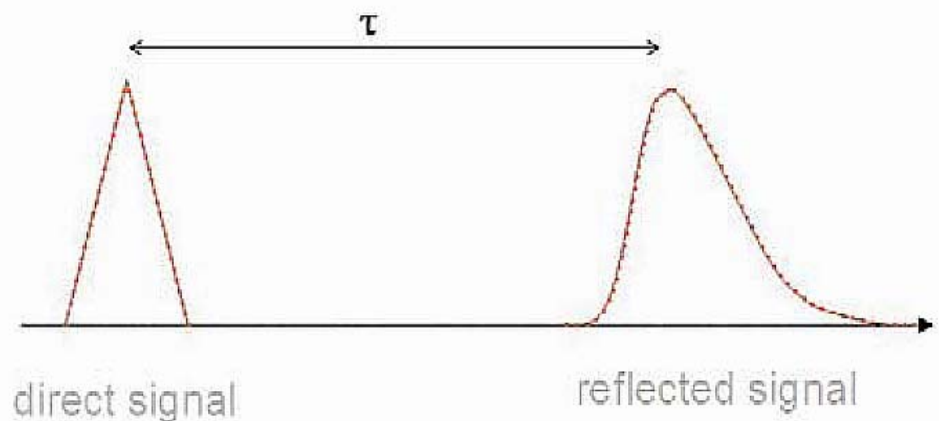
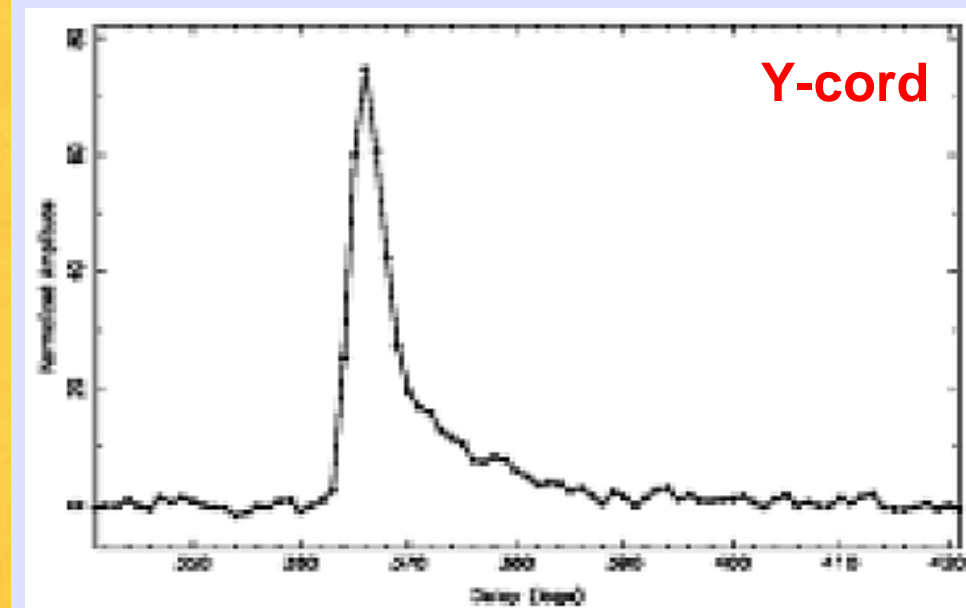
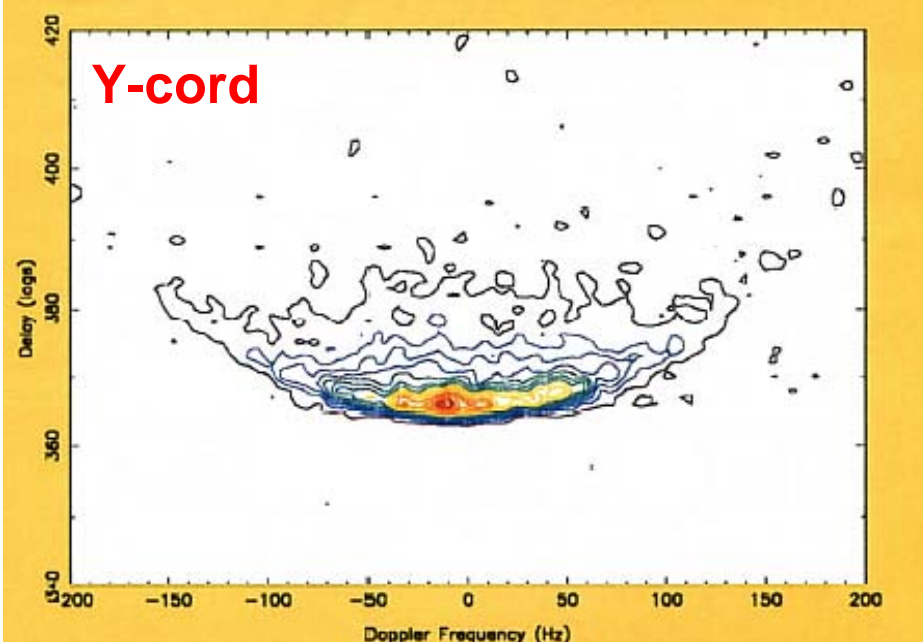
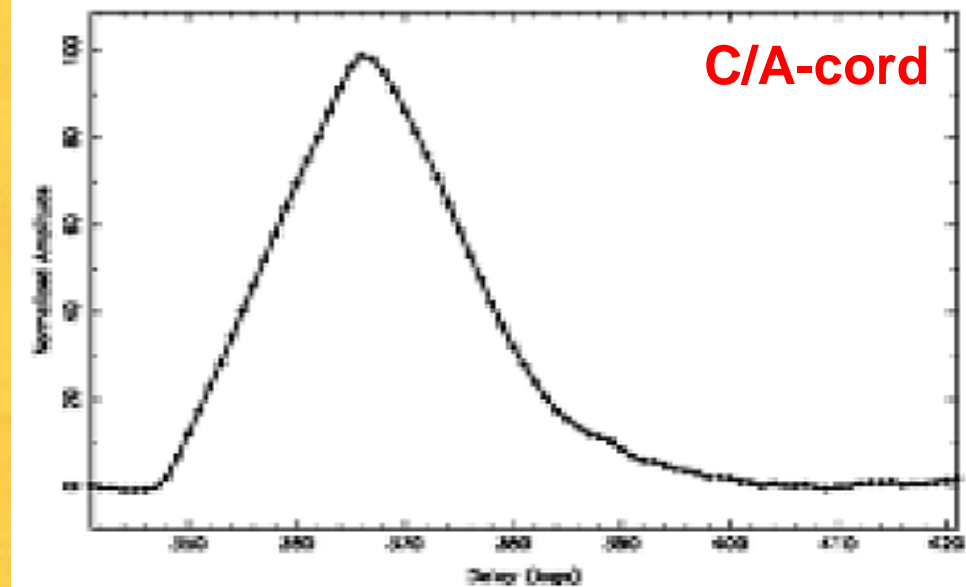
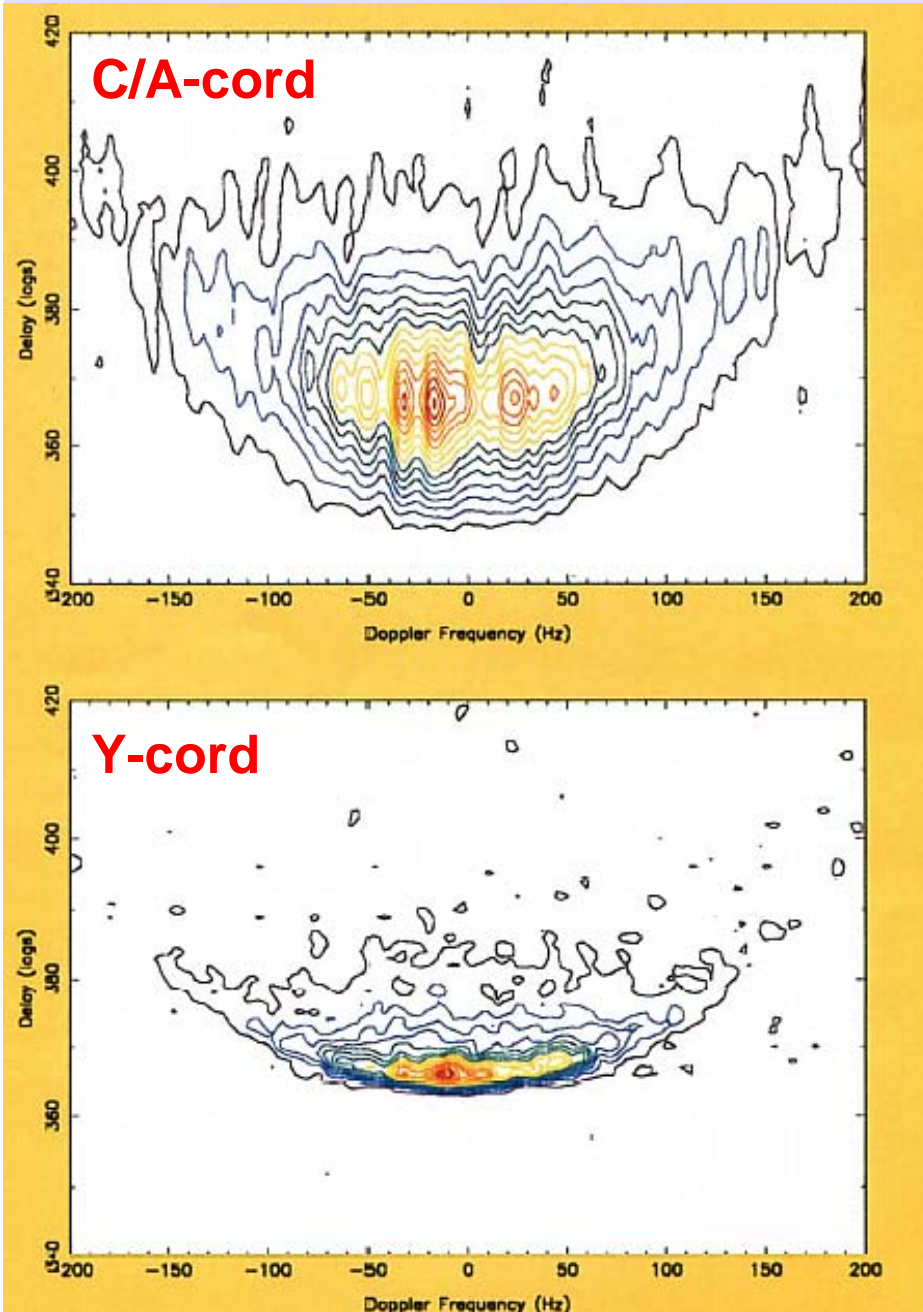


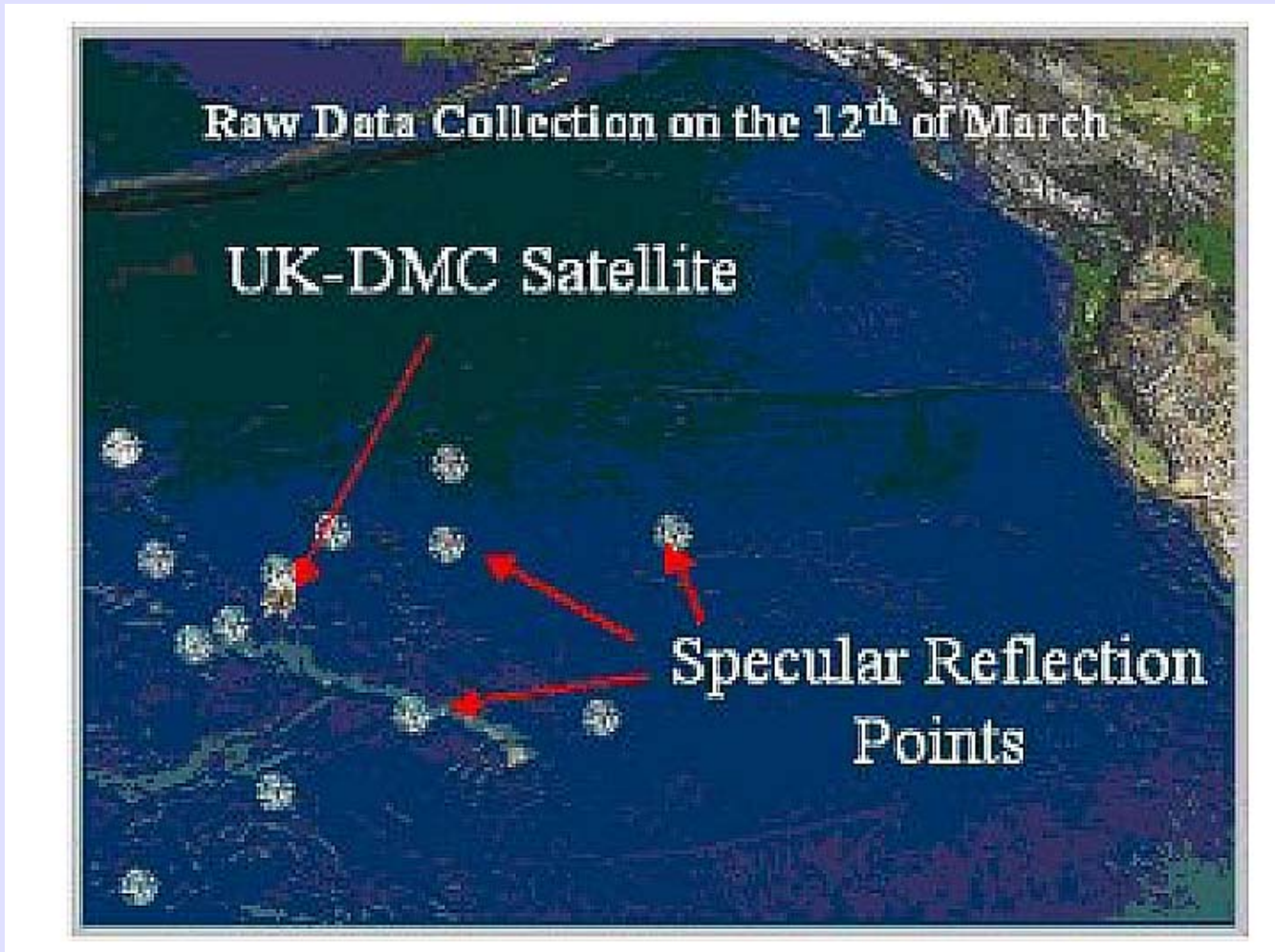
Fig. 18 Delay/Doppler Waveform

Lowe, IEEE Geo.
Remo Sens, 2002



Delay cross-section at zero Doppler

Fig. 19 Data Collection with UK-DMC Satellite March 12, 2004



UK-DMC:United Kingdom's Disaster Monitoring Constellation

Gleason, et al., IEEE Geo Rem Sens, 2005

Fig. 20 Signal Processing

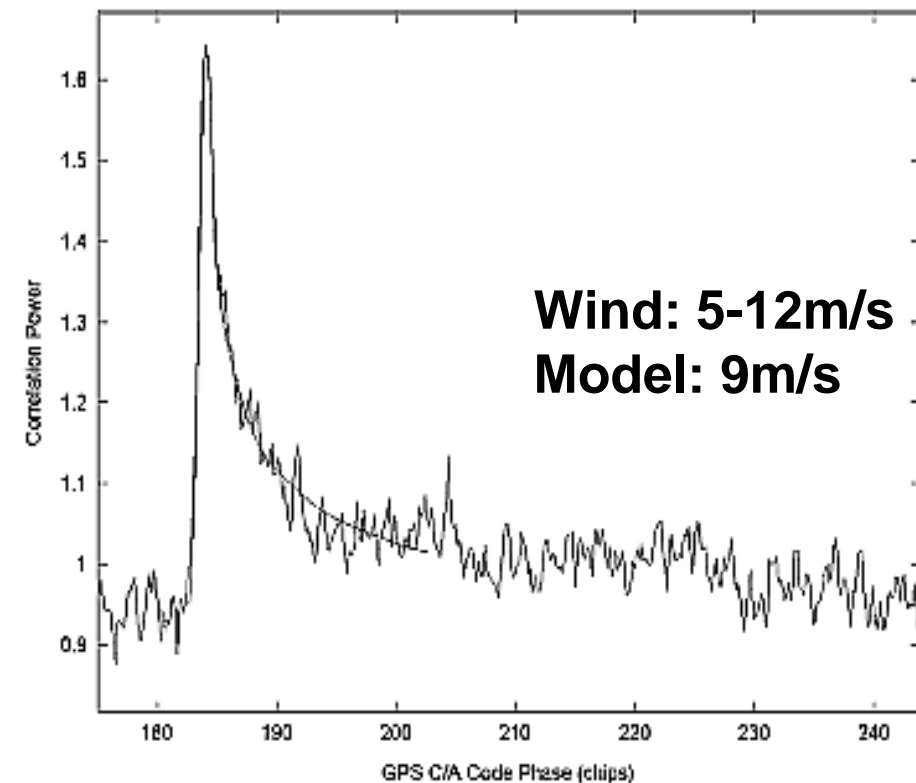
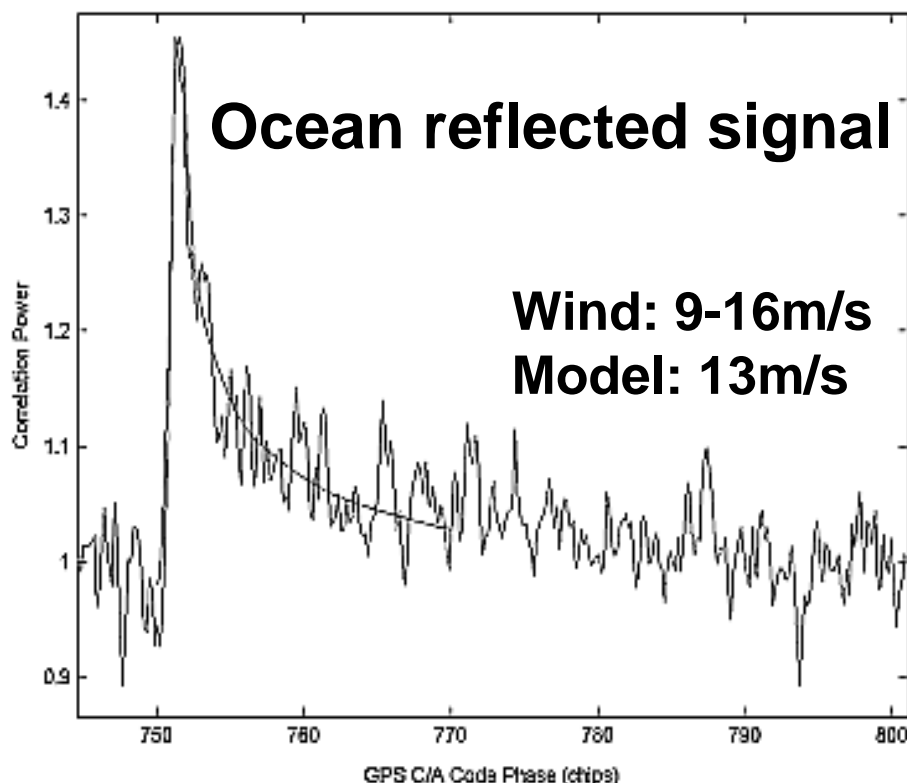
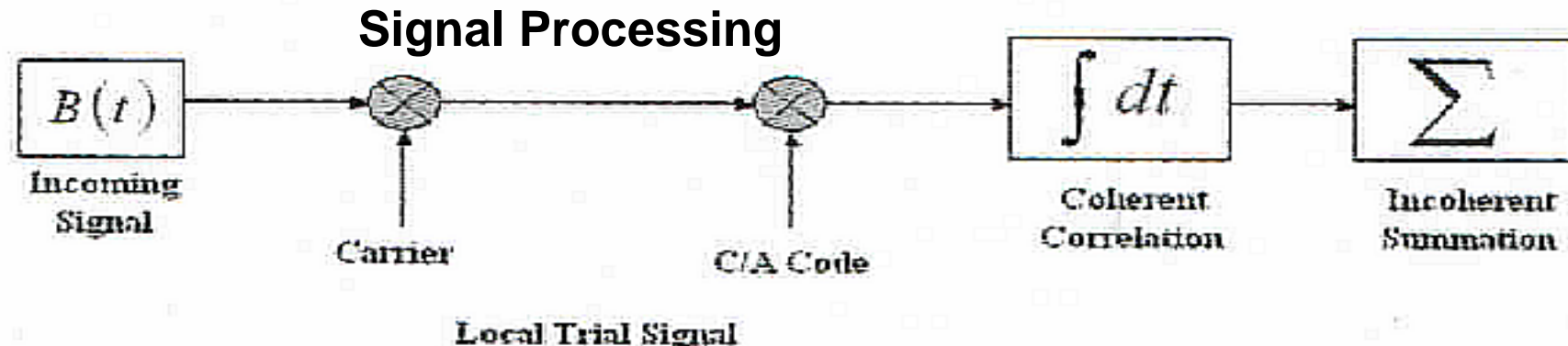
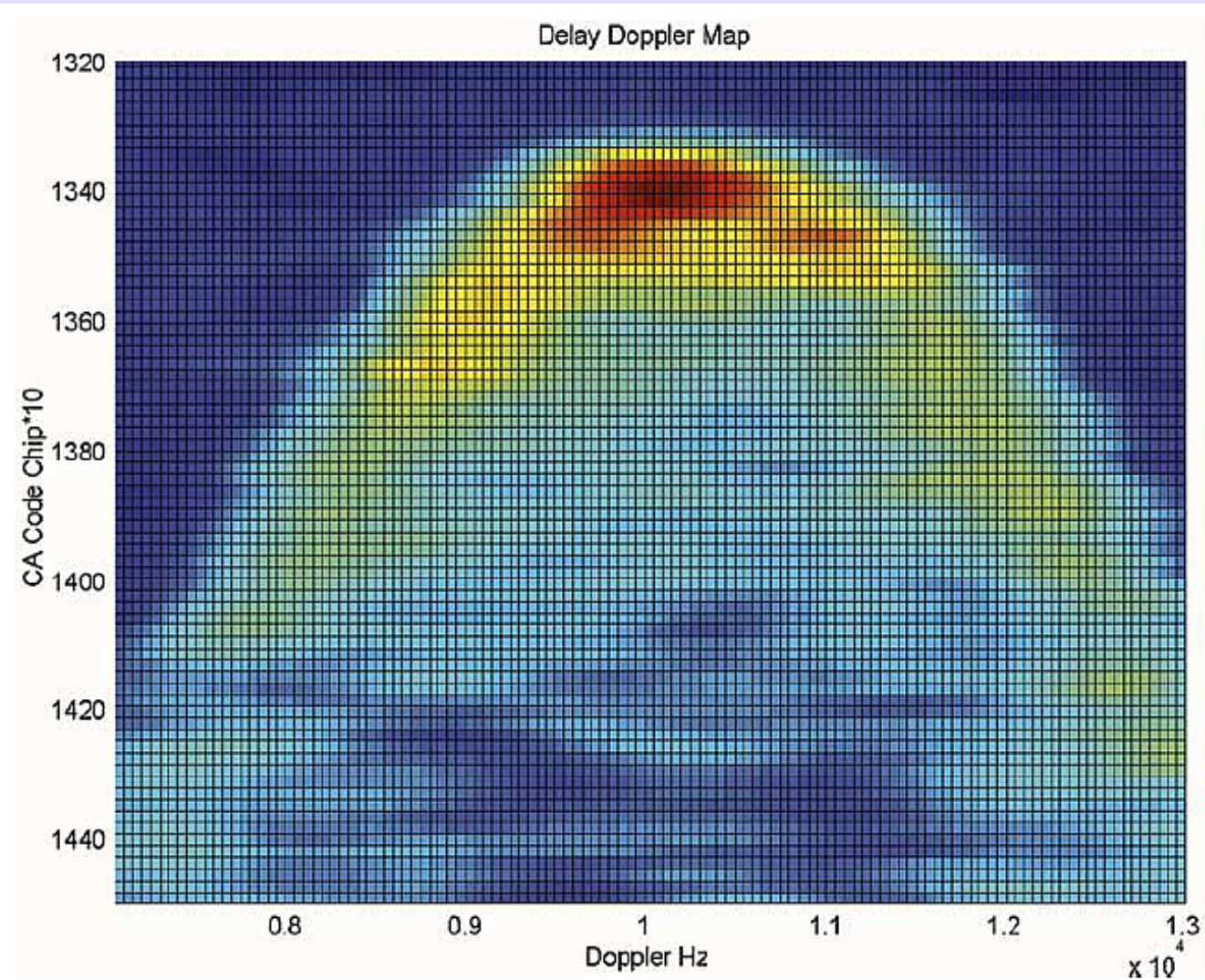


Fig. 21 Delay-Doppler Map of Ocean Reflected Signal of GPS

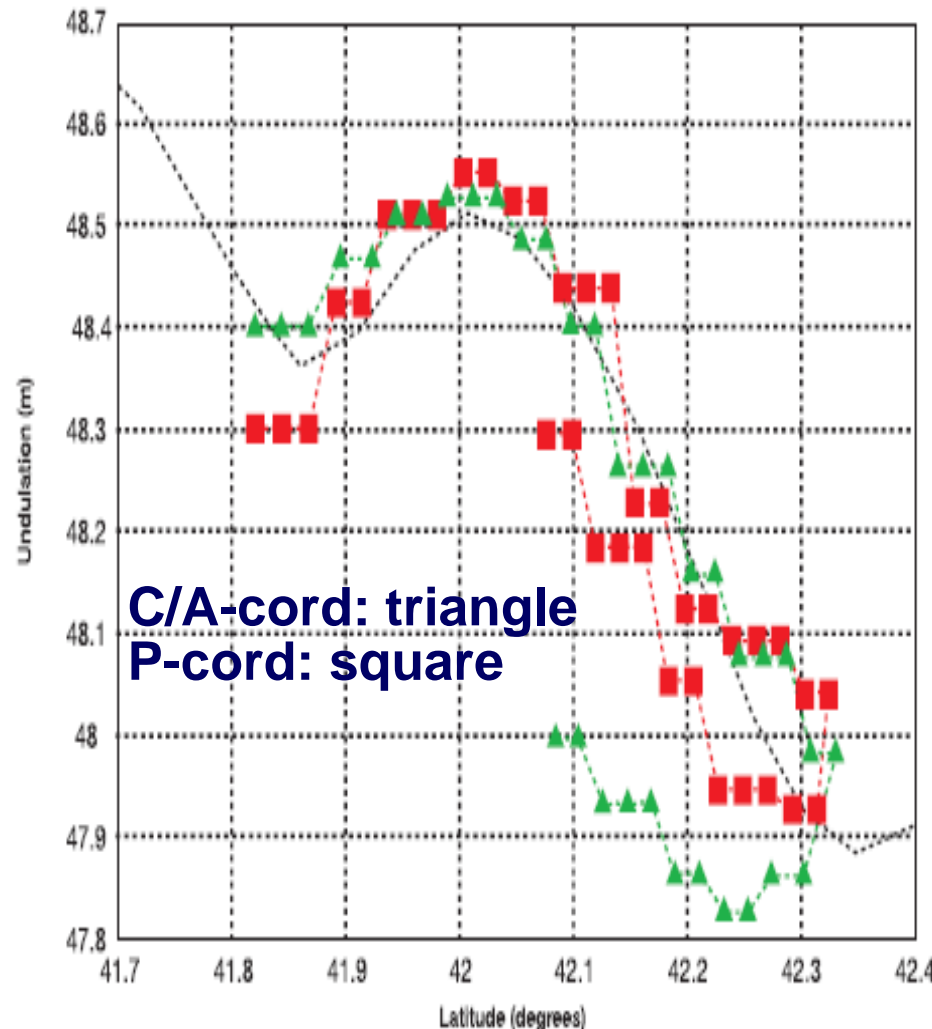


Coherent
Integration:1ms

Incoherent
Summation:1s

Fig. 22 PARIS-Aircraft Test at H1000m over Palamos Canyon

PARIS-Alpha aircraft test



PARIS-Gamma aircraft test

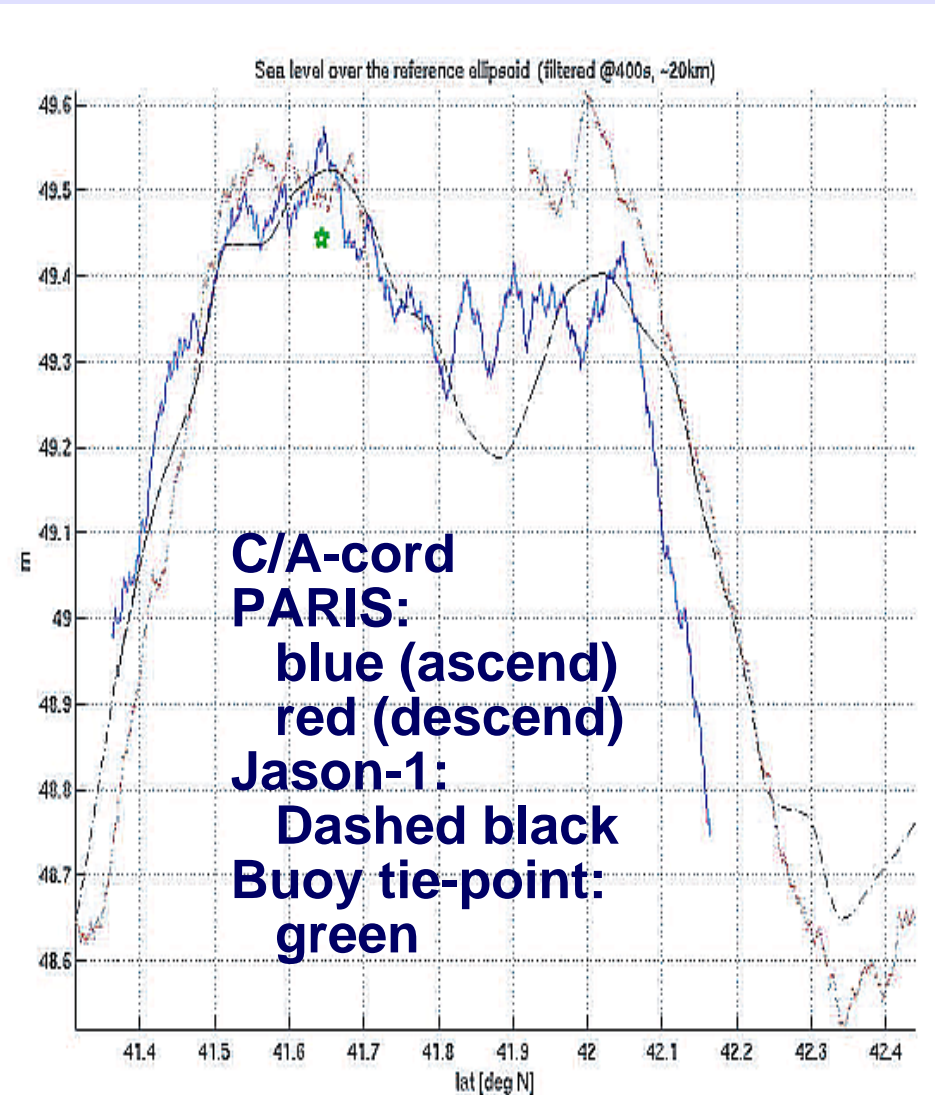
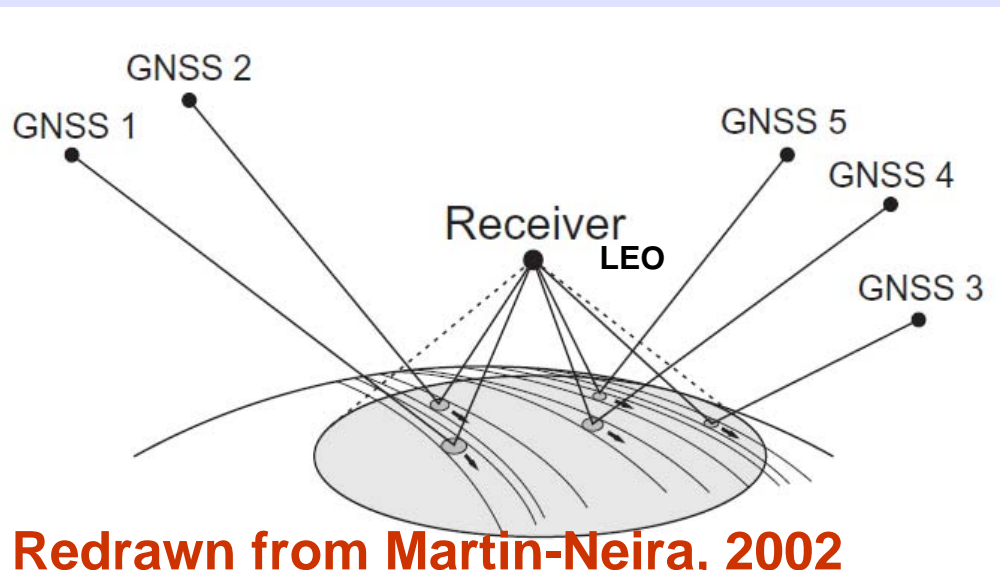
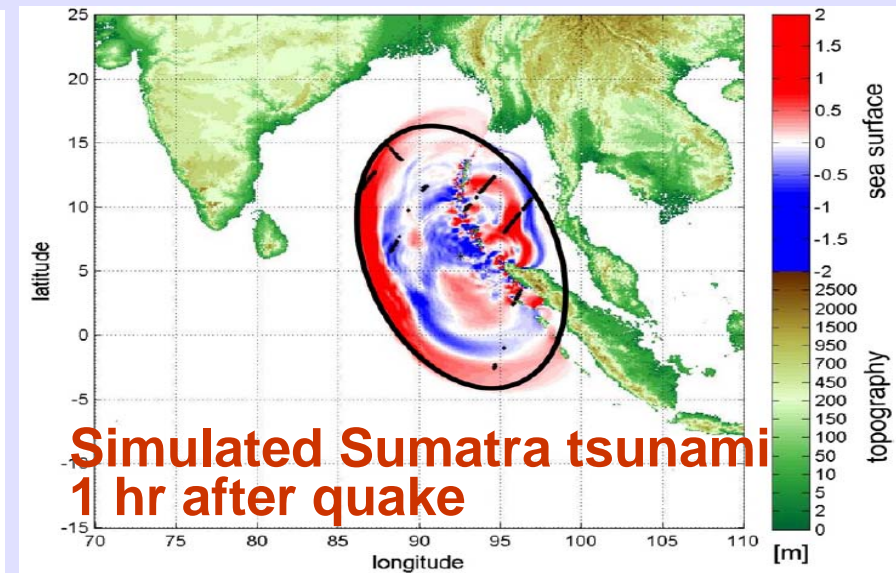


Fig. 23 Tsunami Detection Using GNSS Reflectometry

Stosius, Adv Spa Res, 2011



Redrawn from Martin-Neira, 2002



Detection probability

LEO 18/3:
18-Rx on 3-
orbit planes
GPS: as on
26 Dec. 2004

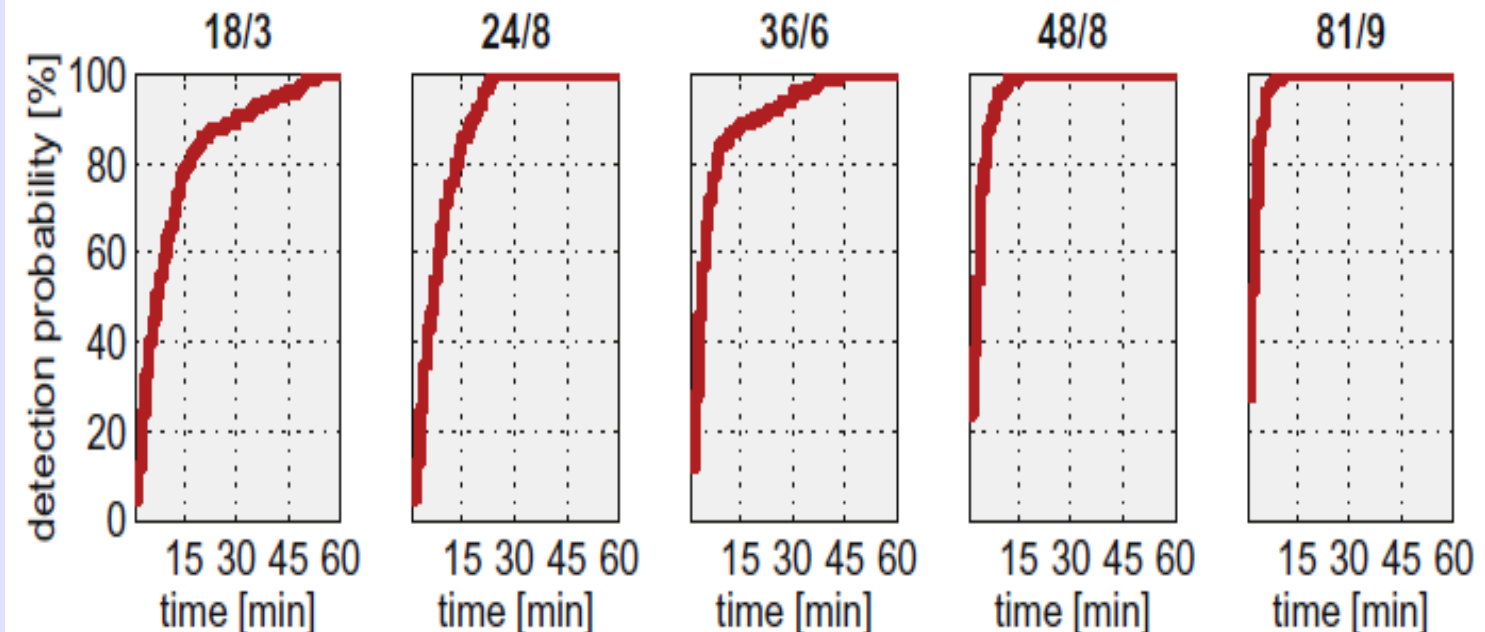


Fig. 24 PARIS-IoD Concept

Martin-Neira, IEEE
Geo Rem Sens, 2011

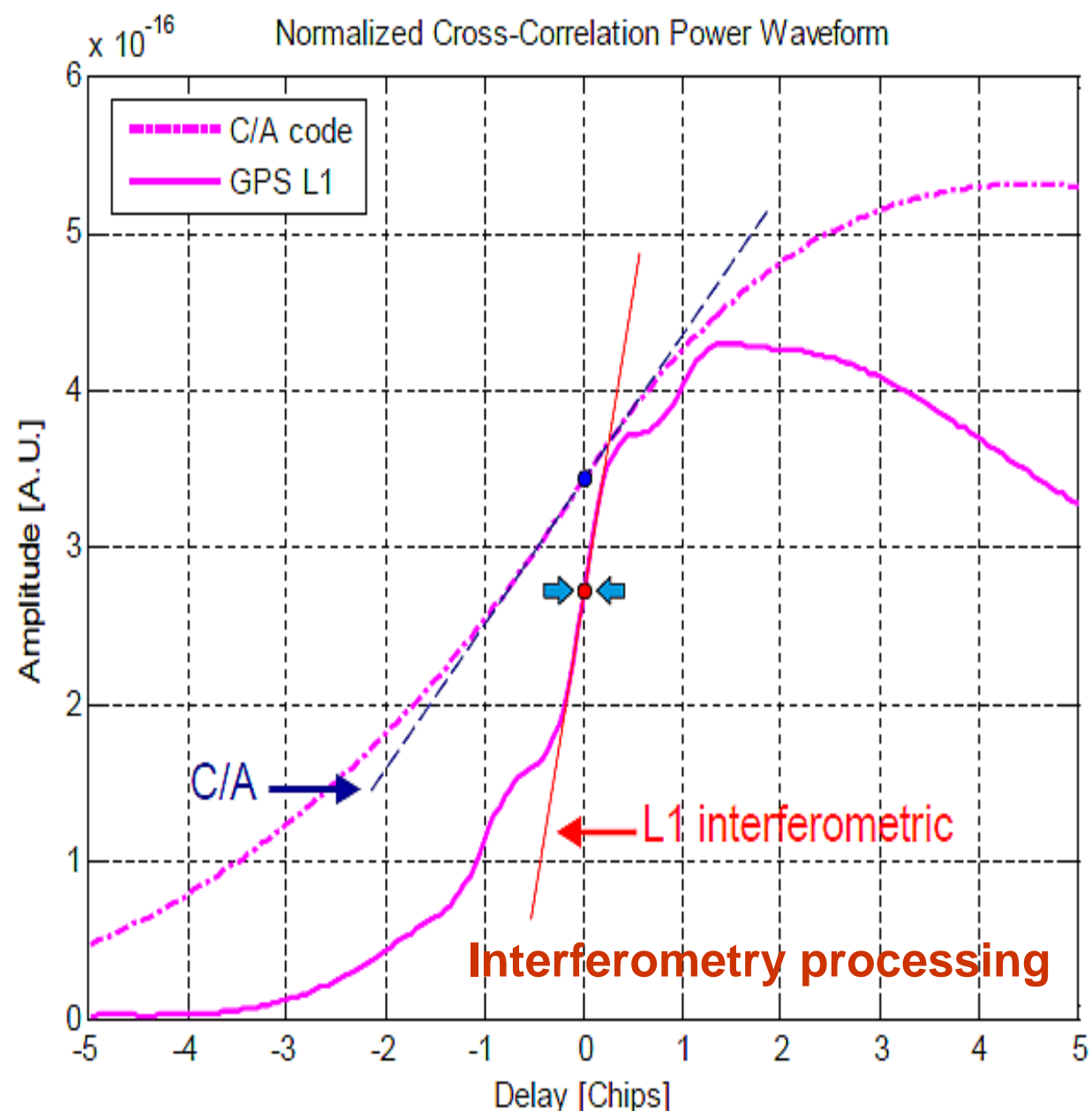
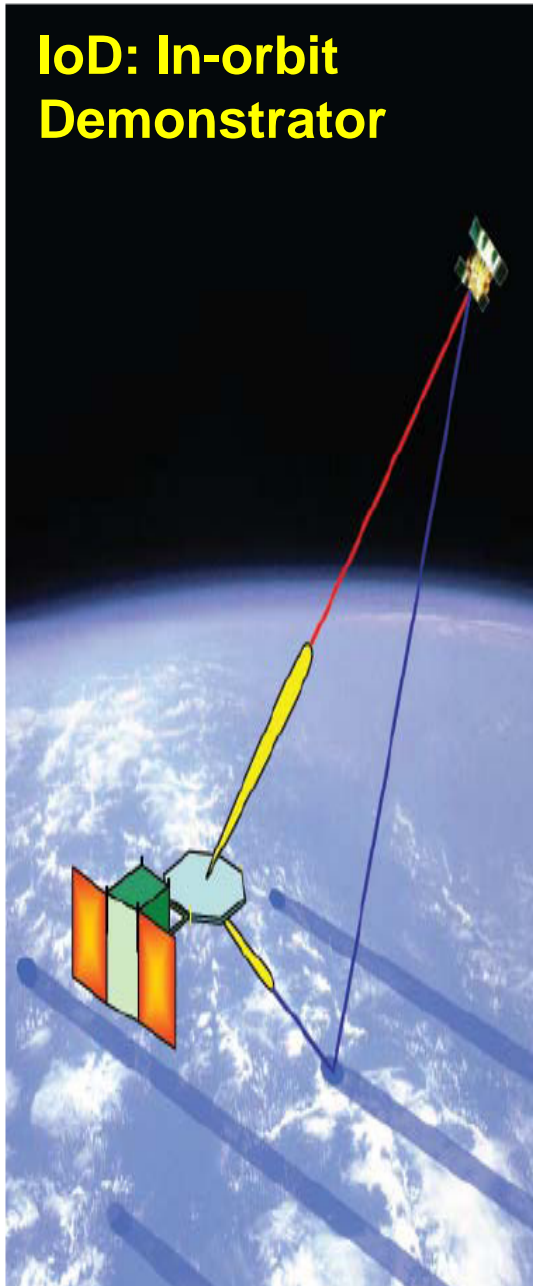


Table 1 Estimated Performance: IoD and Operational Mission

	IOD	Operational
Parameter	Height Accuracy on 100km, G=23dBi, $h=800\text{ km}$	Height Accuracy on 100km, G=30dBi, $h=1500\text{ km}$
Instrument Noise and Speckle	12.5 cm	4.2 cm
Ionosphere	9.7 cm (2 frequencies)	4.8 cm (3 frequencies)
Troposphere (Wet and Dry)	5 cm	2 cm
Electromagnetic Bias	2 cm	2 cm
Skewness Bias	2 cm	2 cm
Orbit	5 cm	2 cm
Total RMS Height Accuracy	17 cm (13 cm at nadir)	7.5 cm (5 cm at nadir)

おわりに

3/11津波のレーダ観測

- merging tsunami

- tsunami signal

スペースセンサの研究

- GNSS-Reflectometry

今後の調査

- 津波の観測報告

- 津波レーダの研究動向

- 津波の早期警戒システムへの取り組み